Numerical Simulation of Chemical Reaction of In-Situ Combustion Using SARA Fraction.

Avwaghwaruvwe Eguono

September 3, 2010

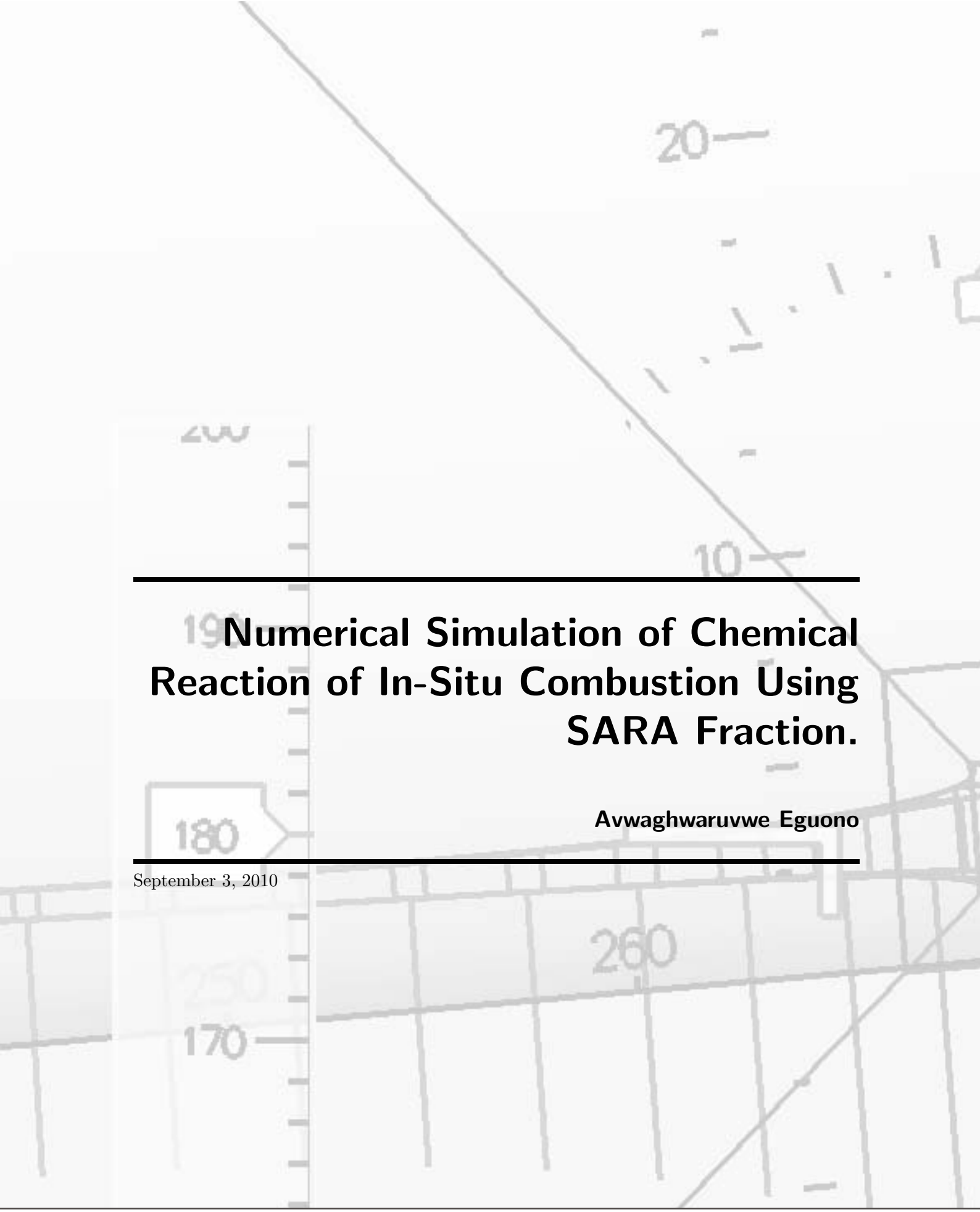

Faculty of Civil Engineering & Geosciences

Delft University of Technology

Numerical Simulation of Chemical Reaction of In-Situ Combustion Using SARA Fraction.

Master of Science Thesis

A thesis submitted to the Department of Geotechnology at Delft University of Technology in partial fulfillment of the requirements for the degree of Master of Science in Petroleum Engineering

Avwaghwaruvwe Eguono

August 2010

Department of Geotechnology · Delft University of Technology

Title	: Numerical Simulation of Chemical Reactions Of In-Situ Combustion Using SARA Fractions
Author	: Avwaghwaruvwe Eguono
Date	: August, 2010
Supervisors	: dr.ir. E.S.J.Rudolph
	: Negar.Khoshnevisgargar
TA Report number	: AES /PE/10-21
Postal Address	: Section for Petroleum Engineering
	: Department of Applied Earth Sciences
	: Delft University of Technology
	: P.O Box 5028
	: The Netherlands
Telephone	(31) 15 2781328 (secretary)
Telefax	: (31) 15 2781189

Dedication

This piece of work is dedicated to God Almighty for the gift of life,His fatherly care,divine provision,protection,grace and strength towards the successful completion of this seemingly challenging period of my master's degree programme.

Acknowledgement

I would like to take this opportunity to express my profound appreciation to Patrick Ogunkunle for his support, and encouragement towards the realization of my long awaited dream of having an MSc degree in a world-class academic university outside the shores of Nigeria. I equally want to appreciate the effort of Adekami Ogidiolu for all his sacrifices support, prayers, encouragement, and for accompany me in the rain to purchase my flight ticket.

Similarly, I would also like to extend my deepest appreciation to my uncle, William Avwaghwaruvwe for his fatherly role, and support toward the success of this programme.

My gratitude also goes to Ochoche Abogonye, and Victor Oshilim for continuous assistance, and keeping in touch on the progress of my studies.

Words are immeasurable for me to express my sincere thanks to my supervisor, Dr.ir.Susanne Rudolph, and Negar for their continuous encouragement, guidance and motivation all through the period of this thesis. Indeed, it was a great opportunity to work and learn from them. Thanks for your warm welcome whenever I need clarification regarding the project. More importantly, for painstakingly reading, and correcting every details of this work. I also want to thank the members of the board of examiners for taking out time to read this work;Cas Berentsen, and Diederik van Batenburg (from Shell International Exploration and Production B.V.).

I also want to extend my profound appreciation to the Geotechnology Section of Delft University of Technology for the partial scholarship, without which I would not be able to fund a much needed postgraduate studies.

Finally, I want to convey my sincere regards to my mother, brothers and sisters, and my fiance (Tammy) for their understanding care, support, prayers and encouragements all through this hectic period of academic pursuit abroad.

Delft, University of Technology — Avwaghwaruvwe Eguono

September 3, 2010

September 3, 2010

Abstract

In situ combustion (ISC) is a thermal recovery technique where energy is generated by a combustion front that is propagated along the reservoir by air injection.Modeling in situ combustion process requires a good description of the crude oil, kinetics data and the chemical reaction scheme. Unfortunately,only limited kinetic data are available on the rates, low temperature oxidation (LTO) and high-temperature combustion reactions (HTO) of crude oils. Moreover, the impact of such data on the modelling of the ISC process has not been investigated thoroughly. In this work,a minimal model (Main base case) of an Athabasca bitumen based on ISC tube experiment was simulated using a commercial thermal simulator (CMG's STARS). The model consists of eight pseudo-components; maltenes, asphaltenes, coke, hydrocarbon gas, carbon dioxide, carbon mono oxide, methane, oxygen, and nitrogen, which are included in the chemical reaction scheme. Analysis of the first results showed that the activation energy of the asphaltene LTO reaction given was too low. Consequently, there was early production of coke at too low temperature.For further study,the activation energy was tuned such that coke production start at 150°C. The cumulative amount produced oil and gas,composition of the gas stream,and the temperature profiles could be qualitatively reproduced successfully.

Furthermore, a more complex description of the crude oil and chemical reaction scheme was adopted. Thereby, the maltene was split up into (saturates, aromatics, and resins),the other components already mentioned above were also included. This SARA based simulation model contains 11 pseudo-components, and eleven chemical reaction. This more sophisticated description of the oil and of the chemical reaction of ISC was introduced to obtain experiments more realistic simulation profiles which are comparable to date ISC tube experiments. The results obtained from the SARA based approach closely match the cumulative oil and gas productions, produced gases, and temperature profiles of the minimum model.

The SARA based pseudo-components model gives more realistic description of ISC of an Athabasca bitumen. The reaction scheme used resembles the actual behaviour better than the minimal model.

Contents

List of Figures

List of Tables

Chapter 1

Introduction

The world continues to rely substantially on petroleum fossil fuels as a primary energy source. Hence there is need for the development of an environmentally friendly alternative source of energy. No attractive economical substitute for crude oil is yet available or is likely to become available in the next couple of decades. While the discovery of new petroleum reservoirs decreases, the need to produce the known reservoirs more effectively increases. So far petroleum accumulations which are relatively easy to be produced, have been utilized. Maintaining the supply of oil to support economic growth in industrial and developing countries requires new and innovative methods in order to unlock the remaining crude oil reserves. A large part of the remaining reserves exist in the form of so-called heavy crude's (10 to 20 API).The development of such reserves by traditional methods (pressure depletion, water flooding) is often inefficient due to the high viscosity of the oil. Thermal recovery processes, which rely on viscosity reduction of the oil through injected heat (steam or hot water) or in-situ combustion, are well suited to unlock heavy oils in an environmentally sound manner [20].

Heavy oil, or extra heavy oil, is a type of bitumen deposit. These sands are naturally occurring mixtures of sand or clay, water and extremely dense and viscous hydrocarbons. These reserves have only recently been considered to be part of the world's oil reserves, as higher oil prices and new technologies allow the profitable exploitation and upgrading to usable products. Oil sands are often referred to as unconventional oil or bitumen [22]

Many countries in the world such as the United States of America, Russia, and some countries in the Middle East have large deposits of oil sands. However, the world's largest deposits occur in two countries; Canada and Venezuela. There oil-sand reserves approximately equal to the world's total reserves of conventional oil. In 2007, 44% of the Canadian oil production was from oil sands, with an additional 18% being heavy crude oil, while the production of light oil and condensate declined to 38%. Because the growth in the production of oil sands has exceeded the decline in production from conventional resources, Canada has become the largest supplier of oil and refined products ahead of Saudi Arabia and Mexico. Venezuelan production is also very large, but due to political problems within its national oil company [1], estimates of its production data are not reliable. Analysts form outside Venezuela believes

Venezuela's oil production has declined in recent years, though there is much debate on whether this decline is depletion-related or not [23].

Heavy oil represent as much as about two-thirds of the world's total petroleum resource, with at least 1.7 trillion barrels ($270 \times 10^9 m^3$) in the Canadian Athabasca bitumens and approximately 235 billion barrels($37 \times 10^9 m^3$) of extra heavy crude in the Venezuelan Orinoco oil sands. The Canadian and Venezuelan deposits contain about 3.6 trillion barrels ($570 \times 10^9 m^3$) of oil in place, compared to 1.75 trillion barrels ($280 \times 10^9 m^3$) of conventional oil worldwide, most of it in Saudi Arabia and other Middle-Eastern countries [11].

Steam drive is one of the most successfully enhanced oil recovery (EOR) method which has been widely applied since the 1960's. However, for reservoirs with a strong bottom aquifer this EOR method is not very well suited because the pressure during production needs to be maintained at or above the aquifer pressure. This is of great importance in particular when the aquifer pressure is high, e.g., higher than or close to the vapour pressure of water, so that the heat released due to condensation of the injected steam is relatively small [2].

Steam-flooding involves the continuous injection of steam with a quality of around 80% to displace the crude the oil towards the producing wells. Cyclic Steam Stimulation (CSS) has been used to produce the Alberta heavy oil reservoir. However; steam flooding is more favourable when the oil saturation is quite high, and the pay zone is thicker than 20 feet. The restriction in the thickness of the pay zone is to minimize heat losses to adjacent formations. Steam-flooding is also limited to viscous oil in high permeable sandstone or unconsolidated sandstone reservoirs. Thus, it is not applicable to carbonate reservoirs. An additional limitation using steam flooding is the fact that about one-third of the oil recovered is consumed to generate the required steam, thus the costs per incremental barrel of oil are high [15].

Steam Assisted Gravity Drainage (SAGD), a quite novel thermal recovery method, allows producing hydrocarbons with a very high viscosity in order of millions of centipoises. Still, the high energy consumption for the steam production is a limiting factor for SAGD.

The thermal recovery process known as in-situ combustion (ISC) has been a source of interest and effort for several decades. ISC is the process of injecting air (or air enriched with oxygen) into oil reservoirs. Part of the crude oil is burnt producing carbon dioxide, steam, coke, and heat which lowers the viscosity of the heavy oil and increases the mobility of the oil. The combustion front moves through the reservoir from the injector towards the producer. Contrary to other thermal recovery processes the main part of the energy required to displace the oil is generated in situ and originates from the chemical reactions between oxygen and fractions of the crude oil. ISC is a combination of various methods such as gas drive, thermal recovery, steam drive and water flooding. E.g. the gas drive is caused by thermal expansion and gas production by chemical reactions[20].

In-situ combustion seems to be economically and technically an attractive process, however the control of this process is difficult. Before application, safety issues such as avoiding uncontrolled oxygen break-through need to be solved. The portion of the crude burnt is likely to be the heaviest and least valuable. In order to control ISC a better understanding of the underlying processes and their impact on the crude oil product is required. In general, ISC classified as a technique that is applicable for (medium) heavy oils because of the dramatic reduction in oil viscosity[20].

In this project, the description of the chemical reactions (LTO and HTO) and their effect on

simulations are studied. The key parameters of the simulations have been identified. Further, the results give insight which degree of complexity is necessary for the description of the oil and the chemical reactions to obtain realistic simulations.

Chapter 2

In-Situ Combustion

2-1 Introduction

In situ combustion (ISC) is an enhanced oil recovery (EOR) method for the production of (medium) heavy oil where energy is generated by a combustion front that is propagated along the reservoir by air injection. ISC has been studied for more than one hundred years, and it has shown promising results at the laboratory scale. The process can be classified as a combination of a thermal method and a gas injection recovery method. The slow moving combustion front is propagated by a continuous flow of air. Starting from the injection well the burned zone is part of reservoir already swept by the combustion front. In the combustion zone injected oxygen reacts with the residual hydrocarbons generating carbon oxide, water, and heat. Hydrocarbons contacted by the leading edge of the high temperature zone undergo thermal cracking and vaporization. Mobilized light hydrocarbons are transported downstream where they mix with the original crude already reducing the viscosity of the oil. The heavy residue of the crude from Low Temperature Oxidation (LTO) reactions, which is normally referred to as coke, is deposited on the core matrix and is the main fuel source for the High Temperature Oxidation (HTO) reactions. Downstream of the vaporization zone is the steam plateau. The steam originates from water formed during combustion and from evaporated formation water. Further downstream the steam condenses because the temperature drops below the steam saturation temperature, and a hot water bank is formed. The leading edge of this bank is the primary area where the oil is banked by the hot water [20]. See Figure 2-1 on page 6.

The ISC process utilizes the two cheapest and most abundant of all EOR injectants; air and water. ISC is believed to be a promising EOR method as it is expected that it can successfully applied in a much wider range of fields than only heavy oil fields, in particular in deeper reservoirs of light or medium oil. However, it is a complicated method with safety and corrosion problems that always need attention. If insufficient coke is deposited from the oil being burned, the combustion process will not be sustained. If excessive coke is deposited, the advancing rate of the combustion zone will be small because the quantity of air required

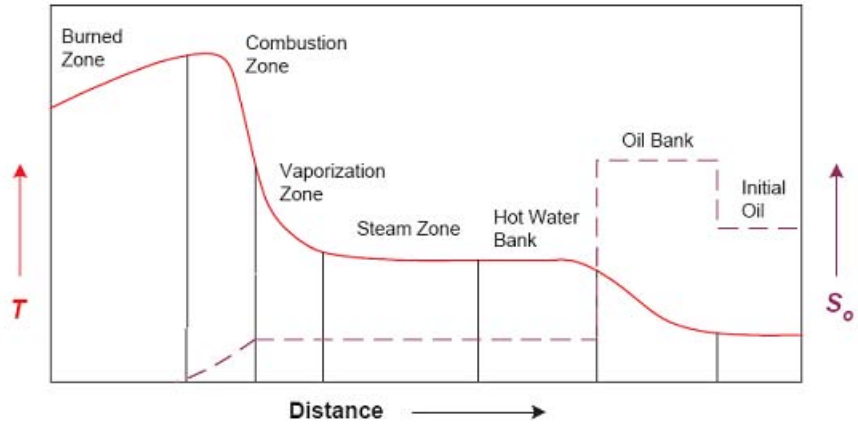

Figure 2-1: Schematic representation of characteristic temperature and saturation distributions in forward in-situ combustion (Not to scale)

to sustain the combustion is high. Therefore, it is important to incorporate oil saturation and porosity in the description of heat losses to the rock [15].

The main purpose of in situ combustion (ISC) in (medium) heavy oil reservoirs is to increase the oil mobility. Heat and gas is produced by burning parts of the oil. The oil downstream is heated due to heat conductivity and the formation and movement of hot gasses. The formation water and lighter components of the oil evaporate and move with the gases produced during combustion through the reservoir. As a result, the reservoir is further heated up; the oil viscosity is reduced due to the temperature increase because of gases dissolved and gas bubbles dispersed in the oil. If the temperature of the oil is high enough (around 350°C) cracking of the oil occurs which also results in a lower viscosity and possibly in evaporation of lighter components. Cracking of oil can also have some negative effects on the sweep efficiency if, e.g., branched hydrocarbons are formed. Their viscosity is commonly higher than the viscosity of comparable normal hydrocarbons. In the end, a combination of all these processes determines the oil mobility [2].

The production of thicker heavy oils by ISC will inevitably face gas override after a period of air injection. Due to this gas override the direction of the in-situ combustion front might get diverted. Therefore, it is important to control the air/oxygen injection rate. Controlling the air injection rate is important for several aspects:

- If the amount of oxygen added to the system is too small, the combustion is not complete and eventually dies.
- If the injection flow rate of the oxygen is small more coke is deposited reducing the effective permeability.
- If too much oxygen is added, the combustion reaction is the limiting step. This might result that not all oxygen is consumed in the combustion reaction so that excess oxygen passes the combustion front reaching the oil further downstream. The temperature downstream is lower so that other reactions (oxygen addition reactions) might be pro-

moted. As a consequence components are formed with a higher viscosity inducing blocking.

If gas override cannot be avoided the conventional, forward dry combustion is not feasible because of the poor volumetric sweep efficiency. In thicker reservoirs with a bottom aquifer, the aquifer can be used to drive the heated oil with a reduced viscosity towards the producer near the oil-water contact. However, the control of this process is even more complicated than the control of the general ISC. Another way to avoid gas override is the co-injection of water into the reservoir. In this way, the heat conduction is improved and the amount of oxygen added can be minimized. This is called wet combustion [2].

2-2 Types of ISC Processes

2-2-1 Dry (forward) combustion

In the forward in-situ combustion process oil is ignited at the injection well and the combustion front is propagated towards the production well by continuous injection of air. As the combustion front progresses into the reservoir, several zones can be identified between the injector and the producer. Figure 2-2 on page 8 gives a schematic representation of the characteristic temperature and saturation zones during ISC. Starting from the injection well the burned zone is part of reservoir already swept by the combustion zone. The burned zone contains the injected the air and possibly a residue of burned fuel. The combustion zone has the highest temperature and this is where most of the energy is generated. Injected oxygen reacts with the residual hydrocarbons generating carbon dioxide, water, and heat. Hydrocarbons contacted by the leading edge of the high temperature zone undergo thermal cracking and vaporization. Mobilized light hydrocarbons are transported downstream where they mix with the original crude. The heavy residue of the crude, which is normally referred to as coke, is deposited on the core matrix and is the main fuel source for the combustion process. Downstream of the vaporization zone is the steam plateau which is formed from water of combustion and vaporization of formation water. Further downstream the steam condenses into a hot water bank when the temperature drops below the steam saturation temperature. The leading edge of the hot water bank is the primary area of oil mobilization where the oil is banked by the hot water [25, 7].

2-2-2 Wet (Forward) Combustion

In the dry forward combustion process, much of the heat generated during burning is stored in the sand behind the burning front and is not used for oil displacement. The heat capacity of dry air is low, and, consequently, the injected air cannot transfer heat from the sand matrix as fast as it is generated. Water, on the other hand, transports heat many times more efficiently than dry air. If water is injected together with air, much of heat stored in the sand can be recovered and transported forward. Injection of water simultaneously or intermittently with air is commonly known as wet, partially quenched combustion. The ratio of the injected water to the air rate influences the rate of burning front advance and the oil displacement behaviour [29].

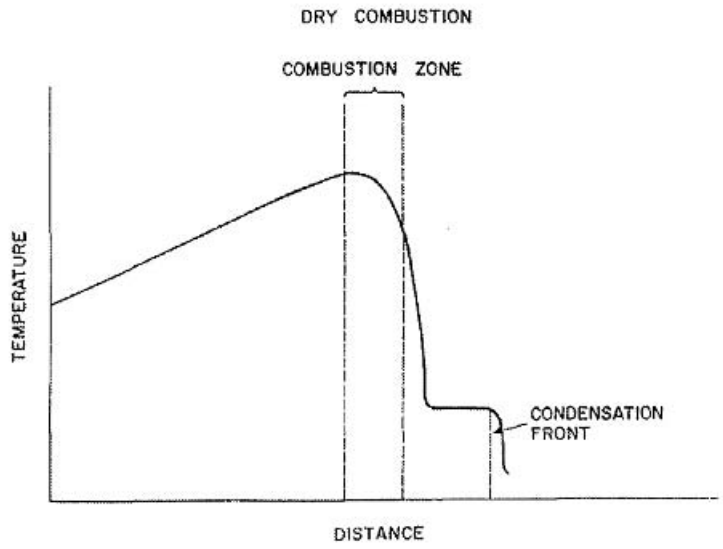

Figure 2-2: Schematic of temperature profile for dry combustion (After Moore et al., 1996)

Laboratory studies and field tests have also shown that water-assisted combustion reduces the amount of oil burnt as fuel. This behaviour increases the amount of oil displaced but, more importantly, it decreases the quantity of air required to burn a certain amount of oil. The mechanism causing the fuel deposit to be decreased during wet combustion is believed to be the increased availability of hydrogen in the combustion zone. A portion of the fuel deposit hydrogenates and becomes mobilized, moving out of the combustion region unburned. The decrease in fuel deposit and air requirement can improve the process efficiency more than 25% [29].

The injected water absorbs heat from the burned zone, vaporizes into steam, passes through the combustion front, and releases the heat as it condenses in the cooler sections of the reservoir. Thus, the growth of the steam and water banks ahead of the burning front is accelerated, resulting in faster heat movement and oil displacement. The size of these banks and the rate of oil recovery depend on the amount of water injected[29].

Wet combustion processes can be classified depending on the injected water-air ratio as "incomplete wet combustion" (Figure 2-3 "normal wet combustion" (Figure 2-4) and "super-wet" or "quenched combustion" (Figure2-5). At low water-air ratios (incomplete wet combustion), the injected water is converted to superheated steam, as it moves toward the combustion front. In this case the injected water fails to recover all the heat from the burned zone. At higher water injection rate (normal wet combustion), the injected water will recuperate all the heat from the burned zone. At even higher water injection rates (super-wet combustion) the maximum temperature at the burning front declines. The operating pressure influences the temperature of the combustion zone during super-wet combustion. The temperature and the saturation profiles for the three modes of wet combustion are depicted in Figures 2-5, 2-6, 2-7 [29].

Quenched (super-wet) combustion is a modification of the wet combustion process that attempts to decrease the air requirement even further. The process does not increase oil recovery, but increases the velocity of the combustion front and reduces compression costs. Water is

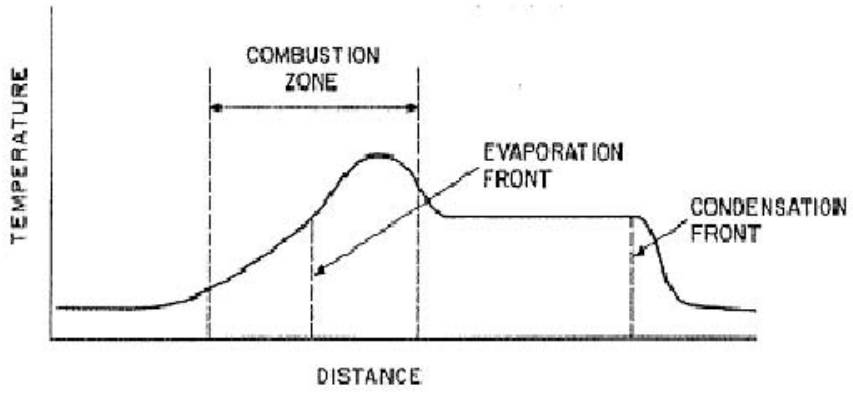

Figure 2-3: Schematic of Temperature Profile for an Incomplete (Partially Quenched Wet Combustion Process (Courtesy of UNITAR Centre, Mehta and Moore, 1996)

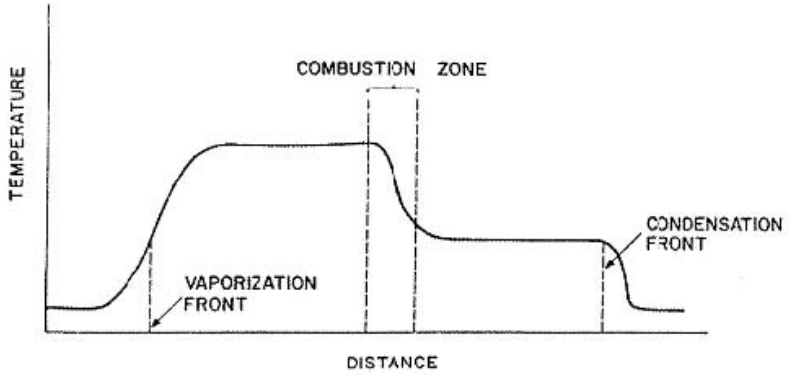

Figure 2-4: Schematic of temperature profile for a normal wet combustion process without convective heat front (Courtesy of UNITAR Centre, Mehta and Moore, 1996)

injected at much higher rates than normal wet combustion. The increased heat, transported by the steam as it passes through to the combustion front, causes combustion temperatures to decrease. The temperature becomes lower than required for burning at the trailing edge of the front so that the oxygen passes through the region without reacting. Therefore, a portion of the fuel deposit is bypassed [29].

Quenched combustion is more applicable in heavy oil reservoirs and less feasible for lighter oils with small amounts of fuel deposits. The process has been patented and field tested by Amoco as the COFCAW (Combination of Forward Combustion and Water flooding) method [6]. Laboratory studies have shown that water rates from 500-1,000 bbl/million scf air result in quenching of the combustion zone and reduce the air requirements. Insufficient field tests have been performed to verify the technical merits of quenched combustion. Cities Service's experience in the Bodcau in-situ combustion project [29, 14] showed that a water/air ratio

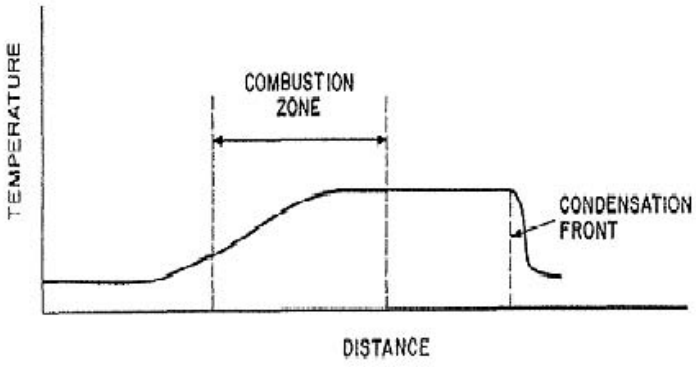

Figure 2-5: Schematic of temperature profile for super wet combustion process (Courtesy of UNITAR Centre, Mehta and Moore, 1996)

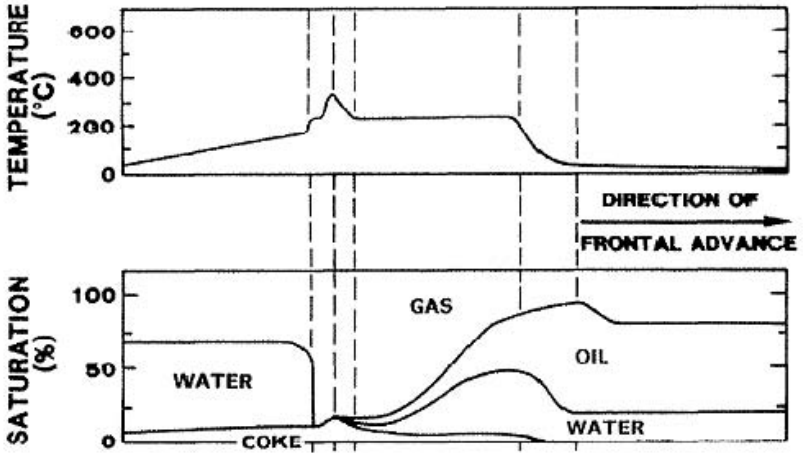

Figure 2-6: Schematic of saturation profile for the incomplete wet combustion process (Courtesy of UNITAR Centre, Mehta and Moore, 1996)

of 250 bbl/ million scf shows improved burning characteristics compared to dry combustion. However, optimum water rates are very difficult to determine because they are affected by reservoir heterogeneities. Segregation of the fluids could result in extinguishing of the fire front and sacrificing of some of the intended benefits of the process. Only operating experience in a particular reservoir will allow selection of the best water/air ratio to maximize recovery and economics [29].

2-2-3 Reverse (inverse) combustion

In heavy oil reservoirs forward combustion is often plagued with injectivity problems because the oil has to flow from the heated, stimulated region to cooler portions of the reservoir. Viscous oil becomes less mobile and tends to create barriers to flow. This phenomenon is especially prevalent in very viscous oils and tar sands. A process called reverse combustion

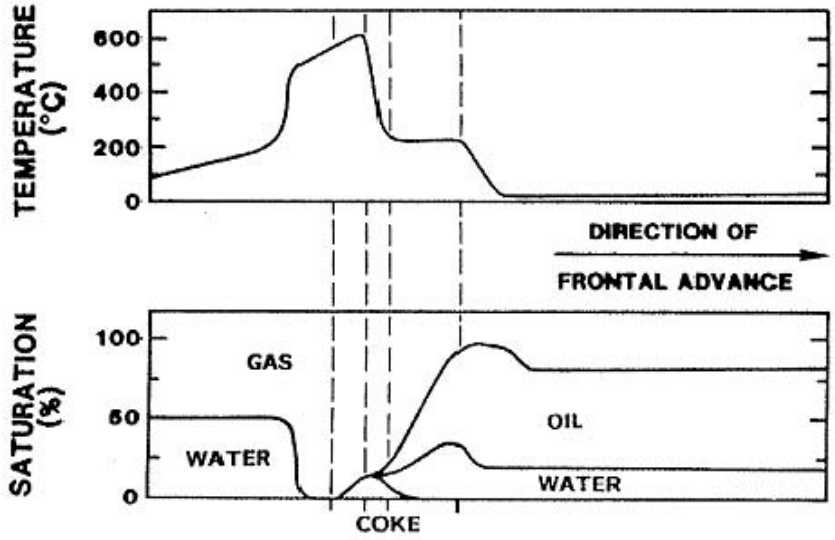

Figure 2-7: Schematic of saturation profile for normal wet combustion process (Courtesy of UNITAR Centre, Mehta and Moore, 1996)

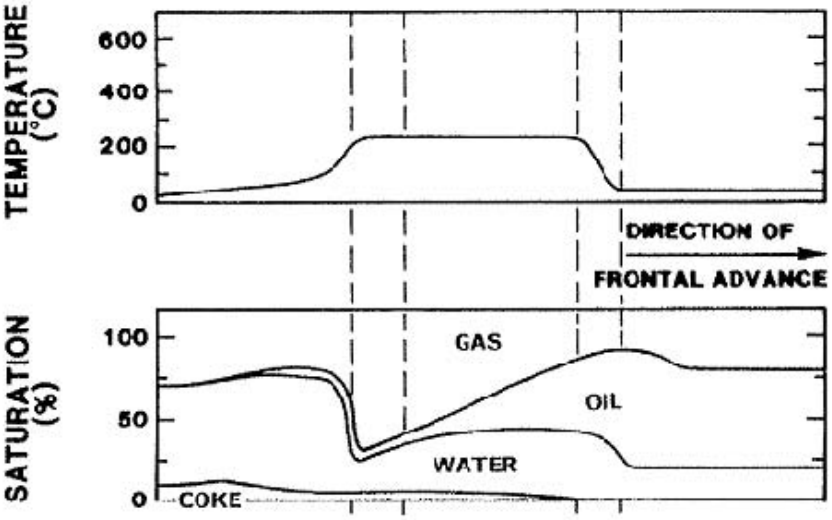

Figure 2-8: Schematic of saturation profile for super wet combustion Process (Courtesy of UNITAR Centre, Mehta and Moore, 1996)

has been proposed and found technically feasible in laboratory tests. The combustion zone is initiated in the production well and moves towards the injector; counter current to the injected fluid flow. The injected air has to travel through the reservoir to contact the combustion zone. The basic concept in reverse combustion is that the major portion of the heat remains between the production well and the oil when it is mobilized. Therefore, once the oil begins to move, very little cooling occurs which would immobilize the oil [29].

The operating principles of reverse combustion are not as well understood as those for the forward mode. Although the combustion process is essentially the same, its movement is not controlled by the rate of fuel burn-off but by the flow of heat. As explained in the section on dry in-situ combustion, the three things required for burning are oxygen, fuel, and elevated temperature. During reverse burning, oxygen is present from the injection well to the combustion zone. The fuel is present throughout the formation. The factor which determines where the burning occurs is the high temperature which occurs at the producing well during ignition. As the heat generated during the burning elevates the reservoir temperature in the direction of the injector, the fire moves in that direction [29].

The combustion front cannot move toward the producer as long as all the oxygen is being consumed at the fire front. Thus, the combustion process is seeking the oxygen sources but can move only as fast as the heat can generate the elevated temperatures [29].

The portion of the oil burnt by forward and reverse combustion is different. Forward combustion burns only the coke-like residue, whereas the fuel burned in reverse combustion is more of an intermediate molecular weight hydrocarbon. This is because all of the mobile oil has to move through the combustion zone. Therefore, reverse combustion consumes a greater percent of the oil in place than forward combustion. However, the movement of oil through the high temperature zone results in considerably more cracking of the oil, lowering its molecular weight. The upgrading process of reverse combustion is very desirable for tar-like hydrocarbon deposits [29].

Although reverse combustion has been demonstrated in the laboratory, it has not been tested in the field [32]. The primary cause of failure has been the tendency of spontaneous ignition near the injection well. However, projects in the tar sands are being considered which attempt to use reverse combustion along fractures to preheat the formation, as the burned zone nears the injection well, the air rate is increased, and a normal forward fireflood is commenced [29].

2-3 Chemical composition of crude oils and pseudo-component

Crude oils consist of a huge number of hydrocarbons and other atoms. 83-87 mol% of the crude is carbon, 10-14 mol% hydrogen and the remaining mol% are components such as nitrogen, oxygen, sulphur, and metals (Ni and V) [29].

Due to the complex composition of crude oils, characterization by the individual molecular types is not possible for performing calculations or simulations. Instead, pseudo-components are defined which are combinations of various hydrocarbon types [3, 5, 8, 12, 17]. An example for this is the definition of the oil composition in terms of maltenes, asphaltenes and coke or the so-called SARA fractions.

For the definition of the composition in terms of SARA fractions, the composition of the crude oil is given in terms of four main chemical groups (see Figure 2-9 for SARA separation scheme) [4].

Saturates: The group of saturates (or aliphatic) are the non-polar hydrocarbons with only single covalent bonds. This includes straight-chain and branched alkanes and cycloalkanes (napthenes). Cycloakanes contain one or more rings, which may have several alkyl side chains. The amount of saturates in a crude oil normally decreases with increasing molecular weight

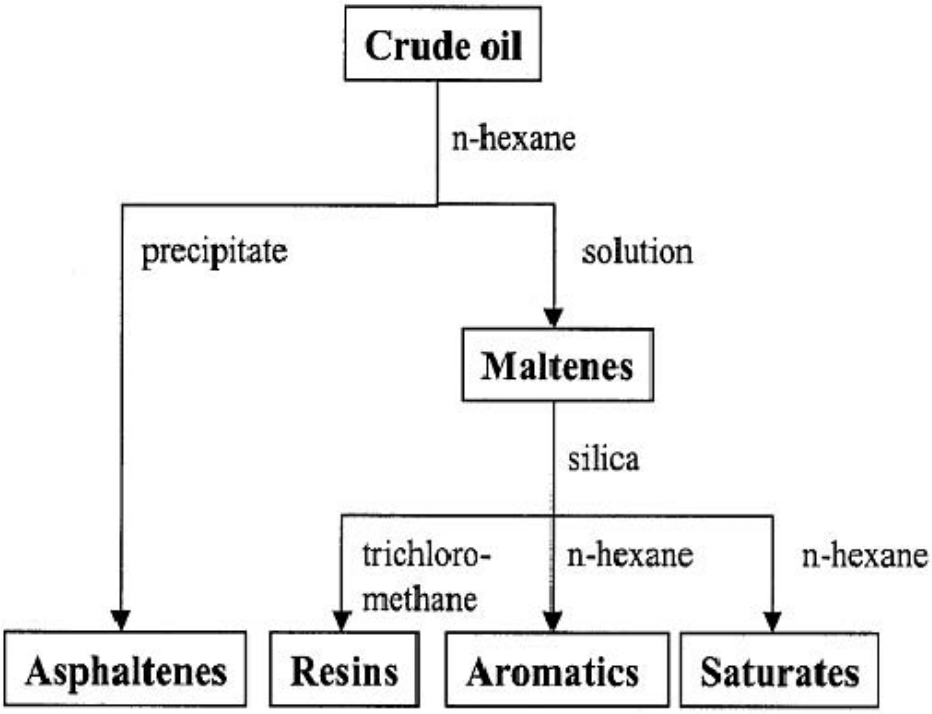

Figure 2-9: SARA-Separation scheme. [31]

fractions. Often saturates form the lightest fraction of the crude oil [4]. Aromatics: The term aromatics refer to benzene and its structural derivatives. Aromatics are common to all petroleum and by far the majority of the aromatics contain alkyl chains and cycloalkane rings along with additional aromatics rings. Aromatics are often classified as mono-, di-, tri-aromatics depending on the number of aromatics rings present in the molecule. Polar, higher weight aromatics may fall in the resin or asphaltene fraction .

Resins: This fraction is comprised of polar hydrocarbon molecules often containing heteroatoms such as nitrogen, oxygen, or sulphur. A common definition of resins is the fraction of the oil which is not a saturate or an aromatic. Resins are soluble in light alkanes such as pentane and heptanes but insoluble in liquid propane. Resins are structurally similar to asphaltenes but have a higher H/C ratio, and lower molecular weight (1000g/mole) [4].

Asphaltenes: Asphaltenes are polar molecules that are similar to resins but with higher molecular weight, typically 500-1500 g/mole. The asphaltene fraction, like the resin fraction, is defined as a solubility class namely the fraction of the crude oil precipitating in light alkanes like pentane, hexane, or heptane. The precipitate is soluble in aromatic solvents like toluene and benzene. The asphaltene fraction contains the largest percentage of heteroatoms (O, S, and N) and organo-metallic constituents (Ni, V, Fe) in the crude oil. The structure of asphaltene molecules is believed to consist of polycyclic clusters substituted with varying alkyl-side chains [30].

2-4 Reaction kinetics

In general, reaction kinetics can be defined as the study of the rate and extent of chemical transformations from reactants to products, e.g., how fast does the chemical reaction occur and how much of the reactant is used. With respect to in-situ combustion the study of the chemical reactions and their kinetics is important for several reasons [29]:

- Characterization of oil reactivity
- Identification of conditions required for ignition; this includes the study if self-ignition is possible in the reservoir upon air injection.
- Characterization of fuel formed by chemical reactions and its impact on combustion.
- To obtain input parameters for kinetic (reaction rate) models used for numerical simulations of ISC processes.

Combustion of crude oil in porous media is a complex sequence of reactions; several consecutive and competing reactions occur in different temperature ranges. Due to the complexity of crude oils, it is impossible to accurately represent all the reactions occurring during ISC. An accurate kinetic representation of all crude-oil oxidation reactions requires an inordinately large number of kinetic expressions and parameters [10]. This complexity is linked to the chemical structure of the individual hydrocarbons. Many of them contain several coexisting C-H bonds which can react successively or simultaneously and often produce intra-molecular reactions. Detailed models for hydrocarbon oxidation reactions are available only for the simplest hydrocarbon molecules and are made up of several reaction steps (equations) [10]. Additionally, even if detailed hydrocarbon oxidation models, exist, they cannot be incorporated into existing in-situ combustion simulators. This is due to up-scaling issues but also because of computer limitations. Detailed oxidation models have been developed and validated only for the simplest model systems. The real situation could not yet be captured in models. Simplified models describing the chemical reactions during in-situ combustion processes have been developed in recent years [10].

2-4-1 Chemical reactions

There are several reactions that occur simultaneously during ISC, and these reactions compete for the available oxygen. These chemical reactions are of two main categories. Oxidations occur in the presence of oxygen, while pyrolysis is caused mainly by elevated temperatures [13]. Several studies have reported three major reactions occur during fire-flooding (ISC);

1. Thermal cracking,
2. Liquid phase low temperature oxidation (LTO),
3. High temperature oxidation reaction (HTO) of solid hydrocarbon residues [13].

Pyrolysis: Pyrolysis is the chemical alteration of hydrocarbons under the effect of heat. The reactions depend on the chemical structure of the oil. These reactions may be dehydrogenation where the number of carbon atoms in the molecule remains the same while the amount of hydrogen atoms decreases, cracking during which larger molecules are 'cut' into smaller molecules with reduced number of carbon atoms, and condensation during which molecules increases the number of carbon atoms. Dehydrogenation is usually predominant for short chain hydrocarbons while cracking is the main reaction for longer chain molecules. At temperatures above 500°C, the products of pyrolysis are light hydrocarbons and a coke-like residue [16].

Thermal Cracking: Thermal cracking reactions are often referred to as the fuel deposition reactions; the carbon-carbon bonds of the heavier hydrocarbon components are broken to form lower carbon-number hydrocarbon molecules plus an immobile fraction which is referred to as coke. In order to better understand thermal cracking reaction mechanisms and to correctly predict product concentrations, it is necessary to understand the thermal cracking reaction within the time frame of the in-situ combustion process [16, 27].

Oxidation: Oxidation can be of two different natures, Low-temperature oxidation and high-temperature oxidation reactions. In general at low temperatures, oxygen combines with the oil to form oxidized hydrocarbons such as peroxides, alcohols or ketones. This generally increases the oil viscosity. At high temperatures it could increase oil reactivity [16].

Liquid-Phase Low-Temperature Oxidation (LTO): The term low-temperature oxidation reaction (LTO) is used to describe liquid-phase oxidation of oils. LTO yields water, and oxygenated hydrocarbons, such as carboxylic acids, aldehydes, ketones, alcohols, and hydroperoxides.The resulting oxygenated oils can have significantly higher viscosities, lower volatilities, and lower gravities than the virgin oils. The temperature range over which these reactions occur extends from the native reservoir temperature up to 300°C. Low-temperature oxidation reactions are either endothermic (chain initiation) or exothermic (formation of oxygenated liquid phase products). LTO may occur simultaneously with bond-scission reactions, which occur in the vapour phase. Because both oxygen addition reactions and bond-scission reactions occur in the same temperature range between 150°C and 300°C, they are referred to as LTO reactions. The transition between the LTO and HTO temperature ranges is characterized by the negative temperature gradient region (NTGR) in which the global oxygen-uptake rates decrease with increasing temperature. This phenomenon has been described in detail by Moore et al. (4). The temperature range, corresponding to the negative temperature gradient region, depends on the oil and the core properties as well as on the operating conditions, e.g., the NTGR temperature range for Athabasca bitumen is approximately between 300°C and 350°C [28, 26].

High-Temperature Oxidation (HTO): The primary products of HTO are carbon oxides and water. The HTO temperature region generally corresponds to temperatures in the range between 380°C and 800°C [16, 26].

2-4-2 Chemical reactions scheme

The overall reaction representing the oxidation of a typical hydrocarbon fuel can be given in the following simplified manner:

$$Fuel + n_1 O_2 \rightarrow n_2 CO + n_3 CO_2 + n_4 H_2 \tag{2-1}$$

Where the stoichiometry coefficients (n_i) depend on the nature of the fuel. This global reaction is a convenient way to average the effects of different (elementary) reactions which actually occur in the reservoir during the combustion process.

This global reaction needs to be split up into smaller chemical reactions. As already mentioned above, the description of the different reactions is quite complex and depends directly on the oil composition and its description. Commonly, the oil description is simplified and reduced to a relatively small number of pseudo-components. The description of the chemical reactions is based on these pseudo-components [29].

For example, Belgrave et al described Athabasca bitumen and the products of ISC in terms of maltenes, asphaltenes, coke, hydrocarbon gas, inert gas, and hydrocarbon gas. The ISC occurs according to the following reaction scheme [33]:

1. Thermal-cracking reactions (first order):

$$Maltenes \rightarrow 0.372\ Asphaltenes \tag{2-2}$$

$$Asphaltenes \rightarrow 83.223\ Coke \tag{2-3}$$

$$Asphaltenes \rightarrow 37.683\ HydroCarbonGas \tag{2-4}$$

2. LTO Reactions

$$Maltenes + 3.431O_2 \rightarrow 0.4726\ Asphaltenes \tag{2-5}$$

$$Asphaltenes + 7.513O_2 \rightarrow 101.539\ Coke \tag{2-6}$$

3. HTO or coke combustion (first order with respect to both reactants):

$$(Coke)CH_{1,13} + 1.232O_2 \rightarrow CO_x + 0.565H_2O \tag{2-7}$$

4. Gas phase combustion (first order with respect to both reactants):

$$Methane + 2O_2 \rightarrow CO_2 + 2H_2O \tag{2-8}$$

$$Gas + 2O_2 \rightarrow 0.9695CO + CO_2 + 2H_2O \tag{2-9}$$

The oil phase was characterized by two pseudo-components; maltenes and asphaltenes, while the solid was represented by coke. The CO_2 and CO production are lumped into one pseudo-component CO with a ratio of $\frac{CO_2}{CO} = 8.96$.

The chemical reaction scheme based on the SARA pseudo-components is given below was used for the SARA based simulation (personally developed).;

Thermal-cracking reactions:

$$Aromatics \rightarrow 0.203\ Asphaltenes \tag{2-10}$$

$$Resins \rightarrow 0.4723\ Asphaltenes \tag{2-11}$$

$$Asphaltenes \rightarrow 153.05\ Coke \tag{2-12}$$

$$Asphaltenes \rightarrow 16.24Gas + Saturates \tag{2-13}$$

LTO Reactions:

$$Aromatics + 1.71O_2 \rightarrow 0.481\ Resins \tag{2-14}$$

$$0.48\ Resins + 1.71O_2 \rightarrow 0.258\ Asphaltenes \tag{2-15}$$

$$Asphaltenes + 13.78O_2 \rightarrow 0.94Saturates + 141.13\ Coke + 2.39HydroCarbonGas \tag{2-16}$$

$$Saturates + 17.62O_2 \rightarrow 14.29CO_2 + 17.56H_2O \tag{2-17}$$

HTO or coke combustion:

$$(Coke)CH_{1,13} + 1.232O_2 \rightarrow CO_x + 0.565H_2O \tag{2-18}$$

Gas phase combustions:

$$Methane + 2O_2 \rightarrow CO_2 + 2H_2O \tag{2-19}$$

$$Gas + O_2 \rightarrow 0.9695CO + CO_2 + 2H_2O \tag{2-20}$$

The main advantages of converting the LTO kinetic model presented by Jia *et al.* [6] to SARA fractions are:

1. It is more comprehensive, since SARA fractions correspond to physical fractions of the bitumen and therefore its fluid properties can be estimated for numerical modelling.
2. Using SARA fractions as pseudo components allow the simulation of heavy oils and bitumen other than Athabasca, since they can be described in terms of SARA fractions. The procedure to separate oils into SARA fractions has been standardized by the American Society for Testing and Materials Standards (ASTM D4124-01).

3. It opens the possibility to simulate different types of crude oils with the same kinetic model, since the reactivity differences among them are expected to be due to their different proportions of SARA fractions.

Strausz and Lown [12, 31] studied the chemistry of heavy oils and bitumen and detailed the chemical structure of each SARA fraction. They elaborate on the reactivity tendencies of some SARA fractions to react with oxygen at low temperatures, with aromatics being the most readily oxidized fraction. Other authors [5] mention the inhibition of oxidation of saturates in the presence of aromatics or resins. Based on this information, the SARA fractions reactivity to oxygen addition reactions, when derived from the Athabasca bitumen, can be expected to decrease in the following sequence. Aromatics>Resins>Asphaltenes>Saturates.

With aromatics being the most reactive fraction of the bitumen, and saturates the least reactive when mixed with other fractions.

2-4-3 Chemical reactions rates

The chemical reactions occurring during ISC need to be described in terms of their thermodynamic equilibrium behavior by the so-called equilibrium constant but also by its kinetic behavior. For the latter the reaction rate is used which describes how fast a reaction occurs and which accounts also for the activation energy of a chemical reaction. The reaction rate can be described for each chemical reaction separately but also for the global reaction. In this case, the reaction rate is represented by an average of all individual reaction rates of the chemical reactions actually taking place [29].

Commonly, the reaction rates of ISC are described by simple reaction rate models accounting for the relation between the fuel and the available oxygen:

$$R_c = \frac{dC_f}{dt} = K P_{O_2}^a C_f^b \tag{2-21}$$

Where C_f = concentration of fuel in kgm^{-3}
P_{O_2}= Oxygen partial pressure Pa
a = Order of reaction with respect to oxgyen partial pressure
b = Order of reaction with respect to fuel concentration

$$k = \frac{(\frac{kg}{m^3})}{(Pa)^a}$$

k= reaction rate constant,

Commonly, “a” ranges between 0.5 and 1.0, while “b” is close to 1.0. The temperature dependency of the reaction rate constant, k , is described by an Arrhenius-type equation,

$$k = A\exp\Big(-\frac{E_a}{RT}\Big) \tag{2-22}$$

The determination of the kinetics of the different chemical reactions occurring during ISC is challenging and often results in non-unique solutions. However, a variety of experimental

techniques can be applied to get values of some of the kinetic parameters such as differential thermal analysis, thermo-gravimetric analysis, accelerating rate calorimetry and effluent analysis [13].

Dubdub et al (1990) investigated the effect of oxygen partial pressure on Athabasca bitumen combustion reactions. They stated that both the extent of low-temperature oxidation (LTO) and the rate of high temperature oxidation (HTO) is affected by the injection rate of oxygen and thus by the oxygen partial pressure [9]. Moore and others (1990) concluded from enriched air combustion tube tests for Athabasca bitumen that at high pressures, the use of oxygen enriched air results in an increased fuel load and decreased burn stability due to the enhancement of low temperature reactions [19].

2-5 Ramped temperature oxidation (RTO) and combustion tube experiments

In-situ combustion tube and ramped temperature oxidation experiments have been used extensively to obtain data for the design of pilot and demonstration projects for enhanced oil recovery by in-situ combustion. Although these are scaled experiments, data such as temperature and fluid production histories are useful in calibrating thermal numerical models for field sensitivity studies. It has been shown that obtained data on the required air injection agree well with field data [21].

Ramped Temperature oxidation tests are conducted under a controlled heating of oil saturated cores (oil-sand mixture) in a flow reactor under a flowing stream of air. The purpose of this test is to study the oxidation behavior and extract reaction kinetics of a rock-oil system under controlled conditions [29].

In a RTO (Ramped Temperature Oxidation) a specified amount of oil is charged to a reactor and the temperature is increased, often linearly with time, while air or oxygen is added to the reactor [33]. The products of the reactions are monitored as the temperature is raised. These experiments are useful to determine self-ignition temperature and kinetic parameters.

RTO experiments are a valuable source of information for the ISC process since they are conducted under a careful control mode and the temperature history, product gas analysis, liquid production and coke yield obtained during the test are measured and recorded. In addition, RTO experiments are run in two identical reactors, with one reactor acting as a reference, which allows distinguishing when the temperature increase in the active reactor is due to oxidation reactions [6], [18].

The second type of experiment is the combustion tube. In this configuration, a packed bed saturated with oil and water is placed in a tube. Combustion starts at one end of the tube and the produced gases, liquids, and temperature along the tube versus time as well as post-experiment coke deposition are examined to understand the behaviour of the combustion zone, reaction kinetics, and fluid transport under combustion conditions. This is essentially a linear one-dimensional (1D) test. Combustion tube experiments are complex and operate at elevated temperatures and pressures and this complicates parameter determination by history-matching experiments given high gradients in component concentrations, temperature profiles, and dependence of parameters on temperature [10].

Furthermore, there is uncertainty associated with up-scaling kinetic parameters to larger size grid blocks that are required for field scale simulation [33].

Chapter 3

Simulator and Main base case description

3-1 Simulator

3-1-1 Description of CMG STARS Simulator

The CMG (STARS) is the Steam Thermal Advanced Reservoir Simulator developed by the Computer Modelling Group in Calgary. It is a comprehensive numerical simulation tool, and has a wide range of simulation applications such as; modelling three phase flow, multi-component fluids, dispersed components (polymers, gels, fines, emulsions, foams), steam assisted gravity drainage (SAGD) and in-situ combustion processes (dry and wet combustion). It can be used to simulate a variety of complex oilfield production and enhancement processes beyond the capabilities of conventional black oil and compositional simulators. Also model laboratory scale projects, pilots, and field scale projects can be described.

3-2 Reservoir and process description

A one dimensional homogeneous Cartesian grid with a length of 1.83 m was used.The total length was split up into 200 grid blocks with the dimension 0.0881m(w)×0.0881m(d)×0.00915m(h) (see Figure 3-1).

Air or air enriched with oxygen was injected from the top; oil was produced from the bottom of the tube grid block(1 1 200). At the first block on top of the combustion tube a heater was used to raise the temperature of the combustion tube to 400°C in the first 15 minutes of the simulation to overcome the activation energy of the ignition. After ignition was established the combustion propagates in vertical downwards direction towards the producer. The initial conditions of the combustion tube are 4100 kPa and 90°C Belgrave *et al.* 1990.

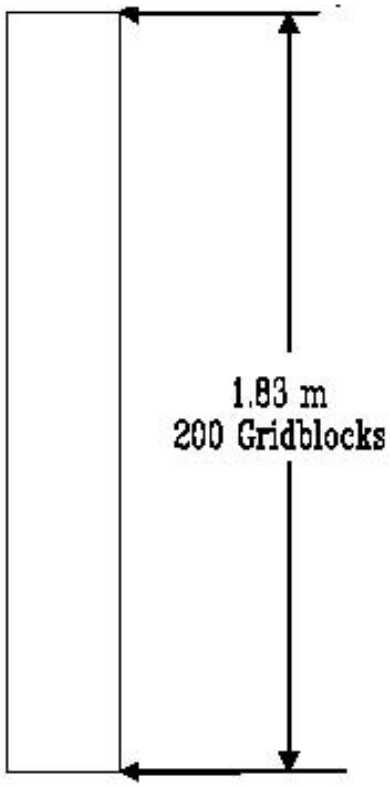

Figure 3-1: One-dimensional simulation model schematic of Yang and Gates

3-3 Main base case description

It was chosen to use combustion tube experiments with Athabasca bitumen as main base case simulation. For this kind of heavy oil extensive experiments have been conducted. The essence of the simulation is to match the simulations to experimental data on the cumulative oil, gas, and liquid productions. In this way, the key kinetic parameters can be identified. These parameters can be used for ISC simulations of other heavy oil or bitumen deposit for which such extensive research has not been done.

3-3-1 Assumptions and general descriptions (Main base case)

The crude is described in terms of the characterization according to Belgrave. The components occur in four phases, namely an liquid oil phase, an aqueous liquid phase, a gas phase and a solid phase. The distribution of the components over the different phases is given in Table 3-1.

It is assumed that the reservoir,and,the overburden and underburden layers have the same initial temperature. In the vertical direction there were no heat losses. The horizontal heat loss parameters are given in Table 3-2. The chemical reaction scheme as discussed in chapter 2 as Yang and Gates models was used (see equation (2-2), (2-3), (2-4), (2-5), (2-6), (2-7), (2-8), (2-9) in chapter 2). The chemical reaction kinetics are described by Arrhenius-type rate relations as explained in chapter 2 (see

Components	Oil	Gaseous	Aqueous	Solid
Water		X	X	
Maltenes	X	X		
Asphaltenes	X			
Oxygen		X		
Nitrogen		X		
Hydrocarbon gas	X			
Carbon II Oxide	X			
Carbon iv Oxide	X			
Methane	X	X		
Coke				X

Table 3-1: Main base case phase distribution of components

Heat Capacity(J/m3 0C)	6.2E4
Thermal Conductivity (J/m day 0C)	6.5E4

Table 3-2: Heat loss parameter in horizontal directions

equation (2-11)). The reaction rates of the chemical reactions given above are described by equation (2-11). The parameters used in the simulations are given in Table 3-3.

Reaction	A	E_a	H_r
Frequency factor	Activation Energy	Heat of reaction	
		(J/mol)	(J/mol)
1	$4.05 \times 10^{10} day^{-1}$	1.16×10^6	0
2	$1.82 \times 10^4 day^{-1}$	4.02×10^4	0
3	$1.18 \times 10^{14} day^{-1}$	1.76×10^5	0
4	$2.12 \times 10^5 day^{-1}$	4.61×10^4	1.30×10^6
5	$1.09 \times 10^5 day^{-1} KPa^{-0.4246}$	5.31×10^4	2.86×10^6
6	$3.88 \times 10^0 day^{-1} KPa^{-1}$	8.21×10^2	4.95×10^5
7	$3.02 \times 10^{10} day^{-1} KPa^{-1}$	5.95×10^4	8.91×10^5
8	$1.31 \times 10^8 day^{-1}$	2.66×10^5	4.44×10^5

Table 3-3: Main base case Kinetic data(Yang *et al.* (2009))

Relative Permeability

For the description of the three-phase flow, the normalized Stone's model was used assuming that water is the wetting phase, gas the non wetting phase and oil is the middle phase. It uses two phase relative permeability parameters to generate three-phase relative permeability data.

The phase imbibitions and drainage curves used in this study are adopted from Belgrave and *et al.* 1990. ISC is a strongly non isothermal process so that also the temperature dependence of the relative permeability needs to be taken into account. The temperature dependence of the endpoint relative permeability was described as shown in Table 3-5

Liquid Viscosity The fluid properties (viscosity) used in the base case simulations are taken

	Oil/Water			Gas/Oil	
S_w	K_{rw}	K_{row}	$S_o + S_w(S_l)$	K_{rg}	K_{rog}
0.05000	0.00000	1.00000	0.07000	0.10000	0.00000
0.10000	0.00039	0.88581	0.16000	0.08615	0.00316
0.15000	0.00156	0.77855	0.21000	0.06632	0.01262
0.25000	0.00625	0.58478	0.31000	0.03711	0.05050
0.35000	0.01406	0.41869	0.41000	0.01881	0.11362
0.45000	0.02500	0.28028	0.51000	0.00829	0.20199
0.65000	0.03906	0.08651	0.61000	0.00296	0.31562
0.75000	0.05625	0.03114	0.71000	0.00073	0.45449
0.85000	0.07656	0.00346	0.80000	0.00011	0.60106
0.95000	0.10000	0.00000	0.95000	0.00000	0.89080
1.00000	0.12656	0.00000	1.00000	0.00000	1.00000

Table 3-4: Relative permeability data(Belgrave *et al.* (1990))

Relative Permeability Curve Endpoints	15°C	800°C
S_{wirr}	0.05	0.00679
S_{orw}	0.15	0.295
S_{org}	0.05	0.350
S_{gc}	0.07	0.0266
K_{rwro}	0.10	0.0508
K_{rocw}	1.00	0.503

Table 3-5: Temperature dependence of the endpoint relative permeability (Yang *et al.* (2009))

from Belgrave *et al.* (1990). The viscosity of bitumen, maltenes and bitumen are described by an exponential function

$$\mu_{bitumen} = 0.48267 \times 10^{-6} \exp(\frac{7685.2}{T}) \tag{3-1}$$

$$\mu_{malt} = 0.19359 \times 10^{-4} \exp(\frac{5369.2}{T}) \tag{3-2}$$

Knowing the viscosities of maltenes and bitumen, the viscosity of asphaltenes was determined from:

$$\mu_{bitumen} = (\mu_{malt})^{x_{malt}} \cdot (\mu_{asp})^{x_{asp}} \tag{3-3}$$

The resulting data were then used to adjust parameters of the expression given below: $\mu_{asp} = 4.892 \times 10^{-25} \exp(\frac{33147}{T})$

Gas Viscosity

The gas phase consists of light hydrocarbon components such methane. They are combined based on STARS equation below; The component viscosity V_{isg} in the gas phase is calculated

from the absolute temperature (T) using

$$V_{isg} = Avg(\mathrm{i}) \times (T^{Bvg\mathrm{i}}) \tag{3-4}$$

$$V_{isg} = \frac{\sum_{i=1}^{numy} V_{isg}(\mathrm{i}) \times y(\mathrm{i}) \times \sqrt{cmm(\mathrm{i})}}{\sum_{i=1}^{numy} y(\mathrm{i}) \times \sqrt{cmm(\mathrm{i})}} \tag{3-5}$$

Equilibrium ratio (K-Value) To describe the vapor-liquid equilibrium the so-called partition or equilibrium constant was used. For the determination of the K-value the correlation given below was used instead of an equation of state.

Gas-Liquid K-Value Correlation $= \left(\frac{k_{v1}}{P}\right) e^{\frac{k_{v4}}{T - k_{v5}}}$ For the description of the heat exchange

Component	K_{v1}	K_{v4}	K_{v5}
Maltenes	1.89×10^7	-6560	-80.1
Asphaltenes	0	0	0
Water	1.18×10^7	-3820	-227
Hydrocarbon Gas	8.62×10^8	-3100	-273
CH4	5.45×10^5	-879	-266
CO2	8.62×10^8	-3100	-273
CO	2.32×10^5	-530	-260

Table 3-6: Main base case gas liquid K-Value (Yang *et al.* (2009))

between gas, liquid and solid, specific heat capacities are used. The temperature dependence of the heat capacities in the different phases is described by correlations as given below. The values of the parameters are taken from Yang and Gates. Gas heat capacity Correlations:$C_{pg}(J/gmol^{\circ}C) = C_{pg1} + C_{pg2}T^1 + C_{pg3}T^2 + C_{pg4}T^3$

Component	C_{pg1}	C_{pg2}	C_{pg3}	C_{pg4}
Maltenes	0	0	0	0
Asphaltenes	0	0	0	0
O2	28.1	-3.68×10^{-6}	1.75×10^{-5}	-1.06×10^{-8}
Hydrocarbon Gas	19.8	7.34×10^{-2}	-5.60×10^{-5}	1.71×10^{-8}
CH4	19.3	5.21×10^{-2}	1.20×10^{-5}	-1.13×10^{-8}
CO2	19.8	7.34×10^{-2}	5.60×10^{-5}	1.71×10^{-8}
CO	30.9	-1.29×10^{-2}	2.79×10^{-5}	-1.27×10^{-8}
N2	31.2	-1.36×10^{-2}	2.68×10^{-5}	-1.17×10^{-8}

Table 3-7: Main base case gas heat capacity (Yang *et al.* (2009)).

Liquid heat Capacity Correlations:$C_{pl}(J/gmol^{\circ}C) = C_{pl1} + C_{pl1}T + C_{pl3}T^2 + C_{pl4}T^3$

Component	C_{pl1}	C_{pl3}	C_{pl3}	C_{pl4}
Maltenes	994	0	0	0
Asphaltenes	2510	0	0	0
O2	46.4	-3.95×10^{-1}	-7.05×10^{-3}	3.99×10^{-5}
Hydrocarbon Gas	-3980	5.25×10^{-1}	-2.27×10^{-1}	3.29×10^{-4}
CH4	-0.02	1.20	-9.87×10^{-3}	3.17×10^{-5}
CO2	-3890	5.25×10^{1}	-2.27×10^{-1}	3.29×10^{-4}
CO	126	-1.70	1.70×10^{-2}	4.19×10^{-6}
N2	76.5	-3.52×10^{-1}	2.67×10^{-3}	5.01×10^{-5}

Table 3-8: Main base case liquid heat capacity (Yang *et al.* (2009))

3-3-2 Main based Case input parameters

The simulation input parameters used are summarized in Table 3-3, 3-4, 3-5, 3-6, 3-7, 3-8, 3-9, A-7 and equations (2-2), (2-3), (2-4), (2-5), (2-6), (2-7), (2-8), (2-9).

Component	Molecular Weight	Critical Temperature Tc	Critical Pressure Pc
	(g/mol)	°C	(KPa)
Maltenes	407	619	1480
Asphaltenes	1090	904	792
Coke	13.1	-	-
Water	18.0	374	22,100
O2	32.0	-119	5050
Gas	43.2	21.9	7180
CH4	16.0	-82.6	4600
CO2	44.0	31.1	7380
CO	28	-140	3490
N2	28	-147	3390

Table 3-9: Molecular weight, critical temperature and pressure of the components included in the simulations (Yang *et al.* (2009))

3-4 Simulations

Three main simulations were performed with enriched air oxygen about 95%;Main base case, with 95% oxygen,base case-1 with a linear oxygen increase from 0 to 95% oxygen with varying temperatures, First SARA simulation with initial main base case kinetic data, and SARA based simulation with adjusted kinetic data.

The base case simulation was a minimum, simple realistic set of components and reactions to represent the ISC behaviour of Belgrave et al,1990 combustion tube experiment, and Yang and Gates,2009 simulation .This simulation model was performed to match, the cumulative productions and temperature profiles as discuss in the results and discussions.Thus,to match the cumulative productions and temperature profiles, the injected end of the combustion tube

Parameter	Value
Numerical grid	$1 \times 1 \times 200$
Grid size	$0.0881 \times 0.0881 \times 0.00915$
Total number of grid blocks	200
Initial water saturation	0.12
Initial oil saturation	0.70
Initial gas saturation	0.18
Initial bitumen mole fraction-Maltenes	0.915
Initial bitumen mole fraction-Asphaltenes	0.085

Table 3-10: Simulation initial conditions and grid blocks (Yang *et al.* (2009)) and Belgrave *et al.* (1990)

Parameter	Unit	Value
Porosity		0.412
Permeability	D	11.30
Rock heat capacity	KJm^3	2280
Rock thermal conductivity	(KJmday °C)	605
Bitumen thermal conductivity	(KJmday °C)	13.40
Water thermal conductivity	(KJmday °C)	58.10
Gas thermal conductivity	(KJmday °C)	4.30
Coke density	$KPa^{-}1$	1380

Table 3-11: Rock and oil properties(Yang *et al.* (1990))

temperature was raised to 400 C for 15minutes to overcome the activation energy, also the activation energy of the asphaltene LTO reaction(see equation (2-6)) was increased. While in the base case-1 simulation, the oxygen content of the enriched air was increased linearly from 0 to 95%,while the nitrogen content decreases form 100% to 5% as described by Belgrave et al,1990.The injected end temperature was been varied.Details of this observed/investigated results are given in results and discussion section.

In the First SARA simulation, the initial base case kinetic data were used without any adjustment in order to investigate the effects on the simulation results. The SARA simulation model was a complex characterization of the oil and chemical reaction scheme as already discussed in the chemical reaction scheme. This was done for better understanding, and to investigate and obtain more realistic reaction kinetics. While in the main SARA simulation, the kinetic parameters of the First SARA simulation were then adjusted to reproduce the base case simulations (see input parameters).

Chapter 4

Simulation results and discussion

4-1 Results and Discussion

4-1-1 Main Base Case

As main base case, the simulations of Yang *et al.* (2009) were chosen. These simulations describe the ISC experiments performed by Belgrave et al 1990, a dry forward ISC with enriched air injection of around 95%. Therefore, first it was investigated if the results of Yang and Gates, 2009 could be reproduced. For this purpose the cumulative production of oil and gas, and the temperature profiles at various locations of the combustion tube are used.

In general the results of Yang and Gates could be reproduced (see also Figure 4-1). However, the results of this work show a slightly higher cumulative oil and lower gas production than compared with Yang and Gates. The cumulative production of oil and gas from this work was $3.950 \times 10^3 cm^3$ and $8.500 \times 10^5 cm^3$ in comparison to $3.750 \times 10^3 cm^3$ and $8.700 \times 10^5 cm^3$ found by Yang *et al.* (2009). These differences can be attributed to the fact that in this work some of the stoichiometric coefficients had to be adjusted in order to reduce the mass balance error.

Figure 4-2 shows the temperature profiles as a function of time at different grid-blocks in the combustion tube. It can be observed that temperatures at various grid-blocks in this work can be compared to Yang and Gates,(2009) and Belgrave *et al.*(1990) combustion tube experiment.

Figure 4-3 shows the cumulative production of the different gases in the combustion tube. They are in good agreement with the simulation results of Yang *et al.* (2009).

Figure 4-4 shows the oil and water saturation, the coke concentration, the oxygen mole fractions, the temperature and the pressure as function of time at middle of the combustion tube at grid-block (1,1,100). Based on this graph it can be explained how the combustion front moves through the combustion tube with time. The behavior observed at this position is in general the same as at other positions in the combustion tube. First, all the properties

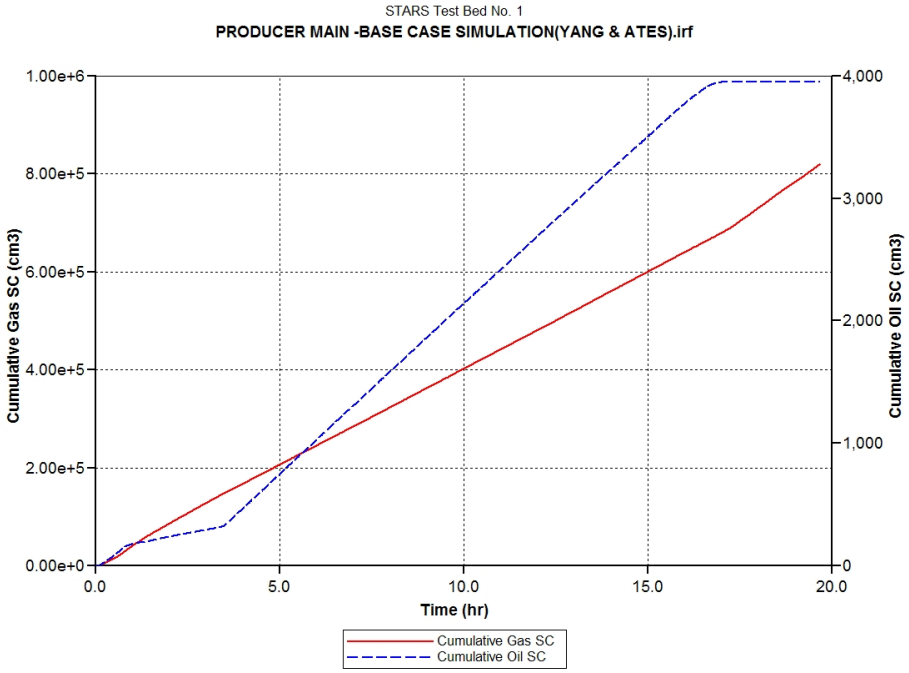

Figure 4-1: Cumulative oil and gas productions profile versus time of main base case.

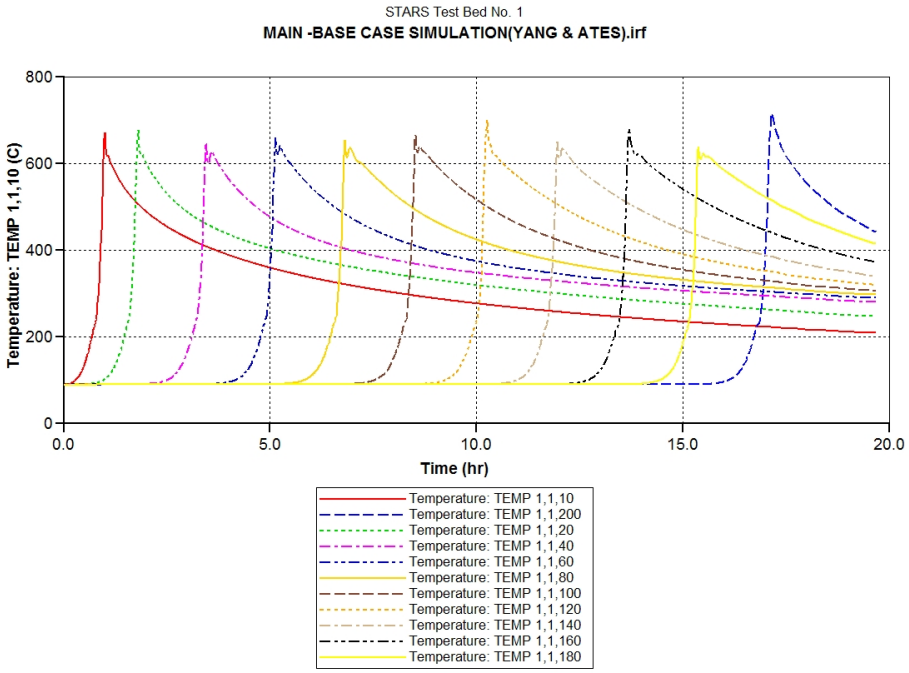

Figure 4-2: Temperature profile versus time of main base case simulations

are in their initial state, the temperature is at 90°C. The water and oil saturation decrease shortly after starting the experiment because of the gas produced further up in the tube, the gas saturation increases. At the same time, the temperature rises slightly up to temperatures

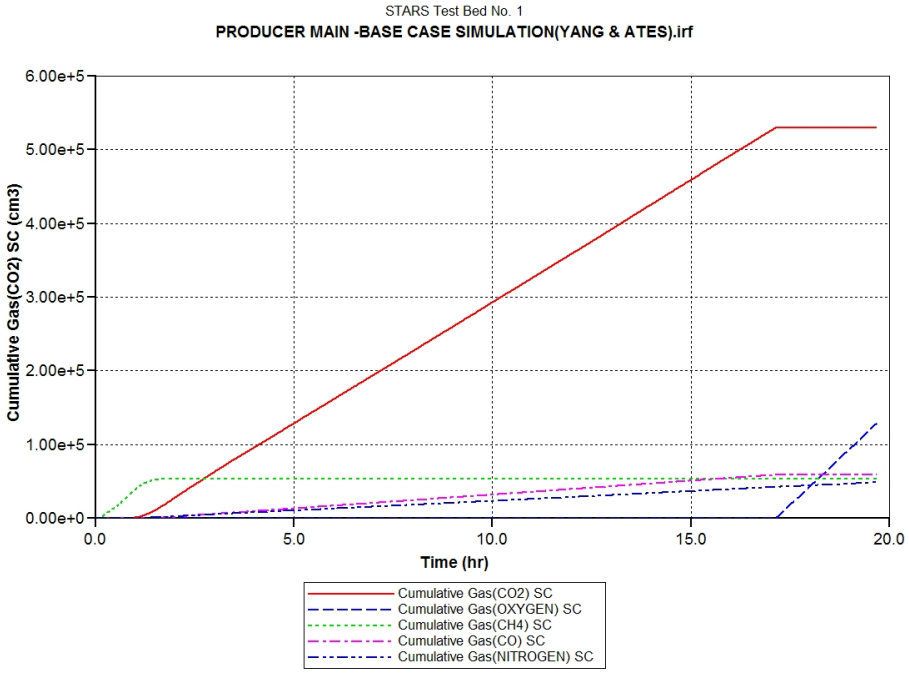

Figure 4-3: Cumulative production profile of different gases versus time of main base case.

around 100°C. Consequently, water evaporates but higher hydrocarbons in the gas stream condensate increasing the oil saturation. The condensation of the gas induces initially a decrease of the pressure. However, the subsequent formation of oil banks results in an increase of the pressure. The slow increase in coke concentration is due to the thermal cracking reaction as described in equation (2-5) in Chapter 2. The injected air is consumed by LTO reactions forming asphaltenes and coke. Some of the oxygen is also used for the gas combustion see equations (2-7),(2-8) in chapter 2 as indicated by the increase of the water saturation and the increase of the temperature. After reaching a temperature of around 380°C the HTO reactions set in and the produced coke reacts with oxygen increasing the temperature even further until all coke has been burnt. After all the coke has been consumed, the oxygen mole fraction stays constant at the value of the injected air. The temperature and the pressure decline to the initial conditions.

Figure 4-5 depicts the oil saturation profile. It can be observed that the oil saturation increases from its initial value of 0.7 up to a value of around 0.8 due to condensation of gases as explained above before it drops to zero indicating the production and the transformation into coke.

Figure 4-6 show the gas saturation profile at different grid blocks, spread over the whole combustion tube with 200 indicating the producing end of the tube and 1 the injection end of the tube. The gas saturation after the combustion front has passed by increases to 100% because in this region the liquid phase was completely transformed either by combustion or evaporation. Initially the gas saturation has its initial value of 0.18. The gas saturation increases due to gas produced up in the combustion tube flowing into the grid block (see also description above). It drops slightly when the heavier hydrocarbons of the gas stream condensate but increases again and stays stable due to water evaporation. The next decline observed is due to gas combustion (see description above).

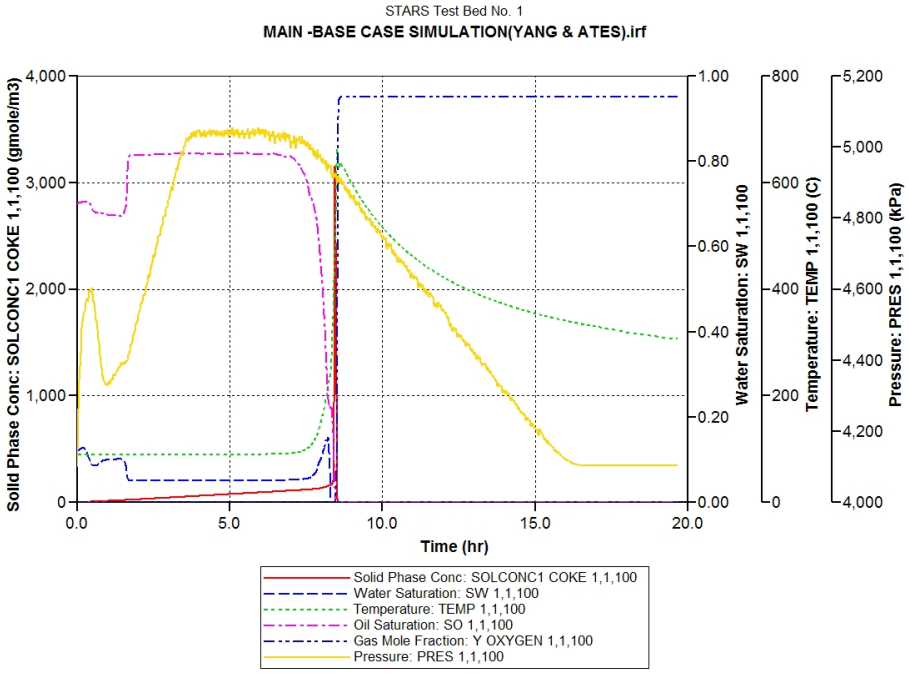

Figure 4-4: Coke concentration, water saturation, pressure, oil saturation, temperature and oxygen mole fraction profile for main base case simulation.

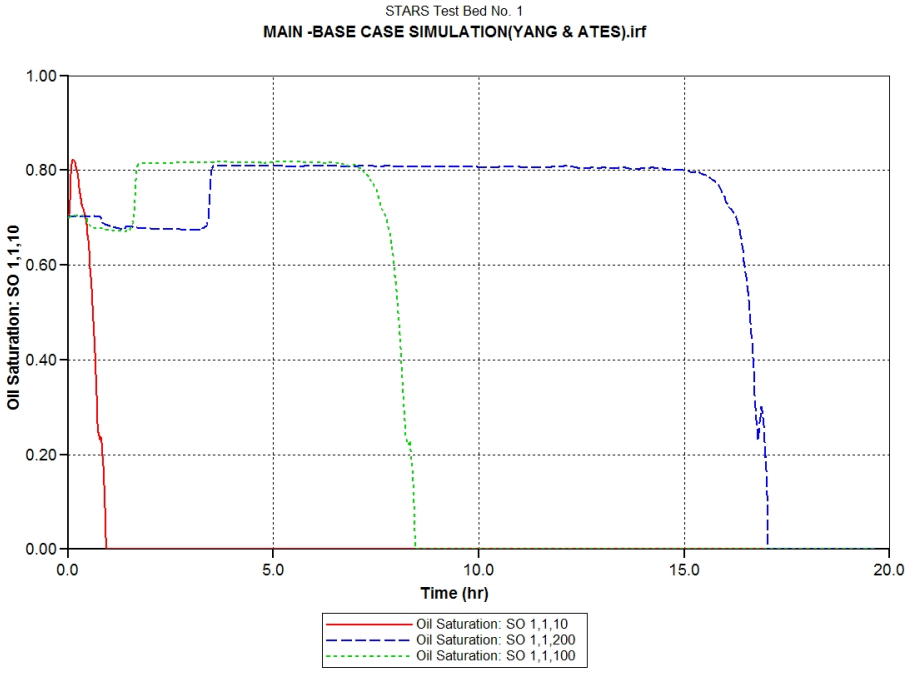

Figure 4-5: Oil saturation profile versus time of main base case

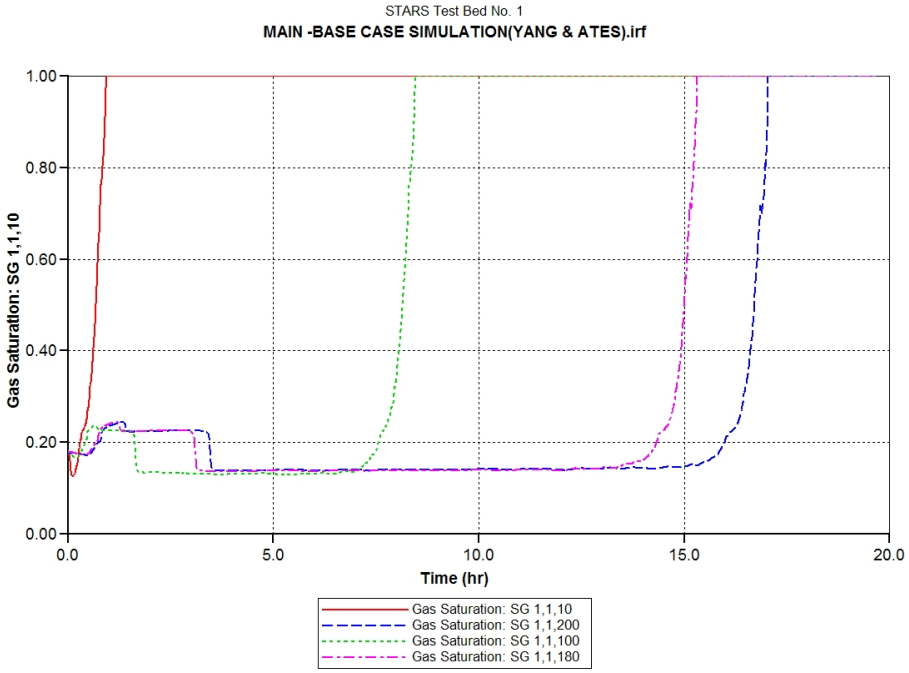

Figure 4-6: Gas saturation profile (at different grid-block) versus time of main base case.

4-1-2 Base case-1

Adjusting the air injection scheme has hardly any influence on the cumulative production of oil and gas compared to the main base case. However, the temperature profile (see Figure 4-7) shows some difference. Now, the highest maximum temperature encountered at a certain position in the tube was found at the producer (the lower end of the tube, block (1, 1, 200)) and was equal to 775°C . Additionally, the time needed to heat up the end of tube was slightly longer for this case than for the main base case. The reason that the maximum temperature encountered at the end of the combustion tube for this simulation is higher than for the main base case is explained by the fact that more coke was deposited for this simulation due to the lower activation energy for the coke producing LTO reaction(see Figure 4-8). If more coke is combusted, more heat is released and thus the combustion tube end is heated more. Consequently, the temperature rises more than for the main base case (see Figure 4-2). This is also supported by the fact that oxygen break-through is observed at a later time (see Figure 4-9).

4-1-3 First SARA based simulation Model

In the next simulation,the oil was described in terms of SARA fractions (saturates, aromatics, resins, and asphaltenes).Due to the different description of the oil,the chemical reaction scheme had to be adjusted too. The simulations now contains 11 pseudo-components and 11 chemical reactions as given in equations (2-10),(2-11),(2-12),(2-13),(2-14),(2-15),(2-16),(2-17),(2-18),(2-19),(2-20). The input parameters are given in Appendix A. The initial kinetic parameters for the 'First-SARA Simulation Model' were calculated from the kinetic parameters of the main base case simulation.

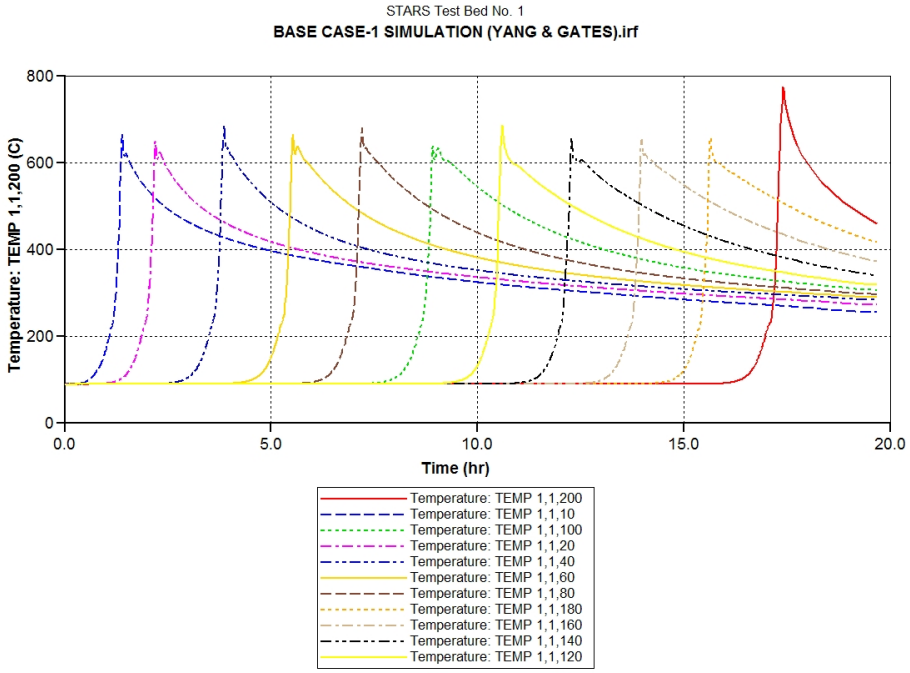

Figure 4-7: Temperature profile versus time of base case-1 simulation

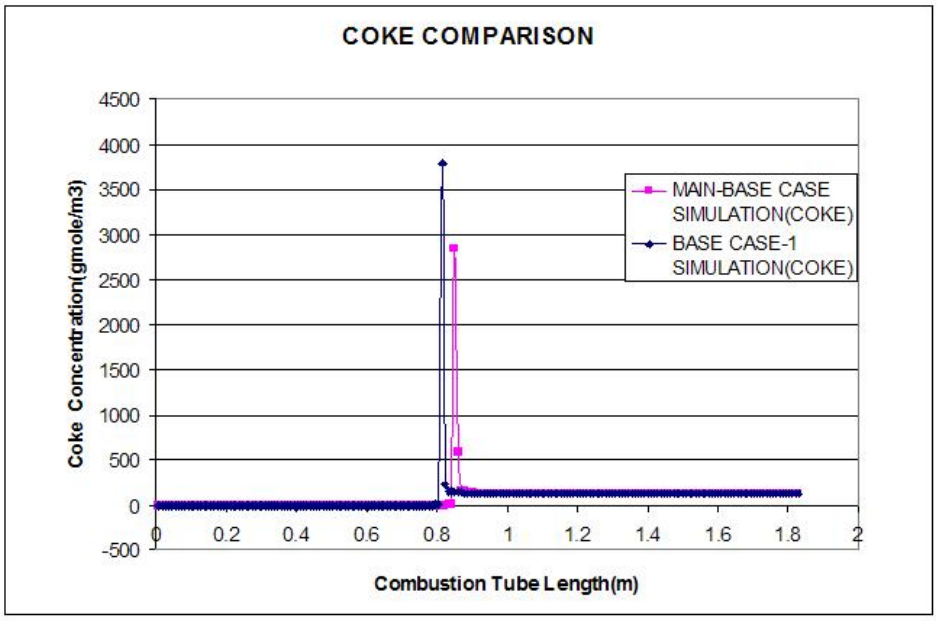

Figure 4-8: Comparison of coke generated profile versus length of combustion tube.

Thereby, e.g., the kinetic parameter for the maltenes of the main base case simulations was split up according to the mass balance into the kinetic parameters of saturates, aromatics and resins (see Table 3-3). Later the kinetic parameters of the SARA chemical reaction scheme were adjusted to match the main base case simulation profiles. These parameters are given in the various tables in Appendix A .

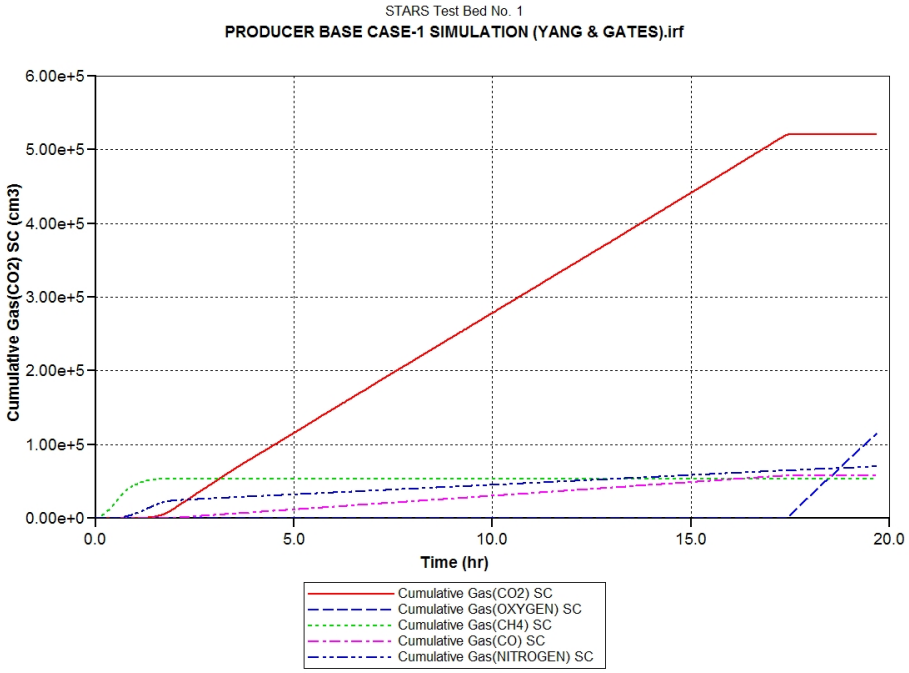

Figure 4-9: Cumulative production profile of different gases versus time of base case-1.

Figure (4-10) shows the cumulative production of oil and gas respectively of the 'First SARA simulation'; in total the amount of produced oil and gas is about the same or slightly more. However, the time needed to produce the oil is less than observed in the main base case. In the main base case it took 17 hours to reach a constant cumulative oil production, while now it takes 12.5 hours. Consequently, the oxygen break-through is observed earlier, namely after 12.5 hours (see Figure 4-12). However, the cumulative (hydrocarbon) gas production has not been affected.

Figure 4-11 shows the temperature profiles at various locations in the combustion tube as a function of time. We can see that the maximum temperature reached at the top of the tube (close to the injector) are the highest, decreasing towards the middle of the tube before they increase again towards the producer, e.g., the temperatures in blocks (1 1 10), (1 1 20), and (1 1 200), are 745 °C , 684 °C , 623 °C respectively. The reason for this is that already at low temperatures, and thus also at the top of the tube, coke is produced due to the chosen kinetic parameters (see Figure 4-13). This coke is then combusted causing these high temperatures which is supported by the increase of carbon dioxide concentration (see Figure 4-12). The formation of coke at these low temperatures and the subsequent combustion is a result of the way how the kinetic parameters were defined for this first SARA simulation.

The results of this simulation clearly document that the description of the oil and accordingly,the reaction scheme have impact on the simulation results. In particular, the results are sensitive to the choice of the kinetic parameters.

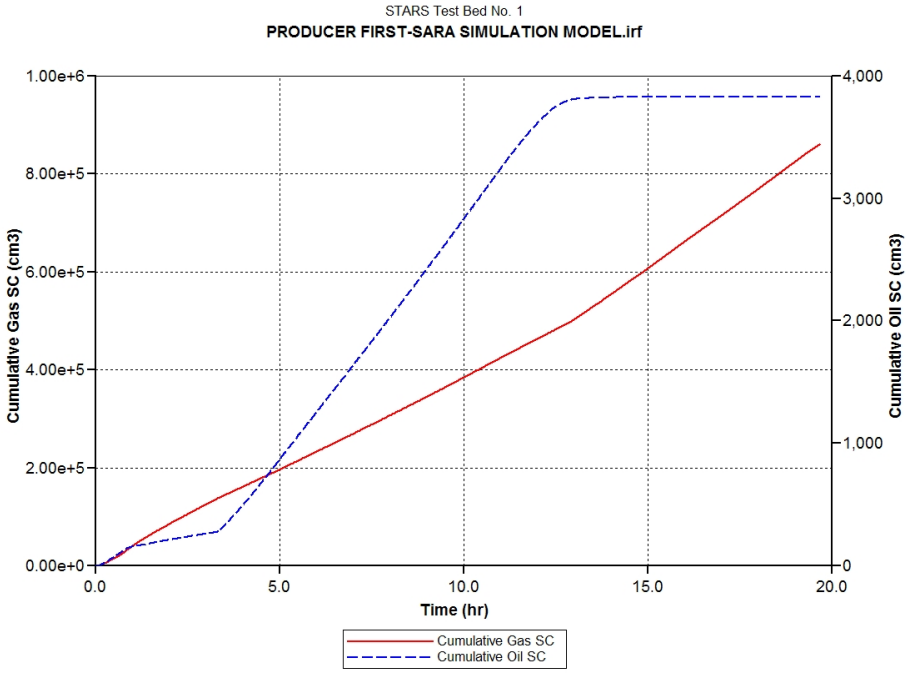

Figure 4-10: Cumulative oil and gas productions profile versus time of first SARA.

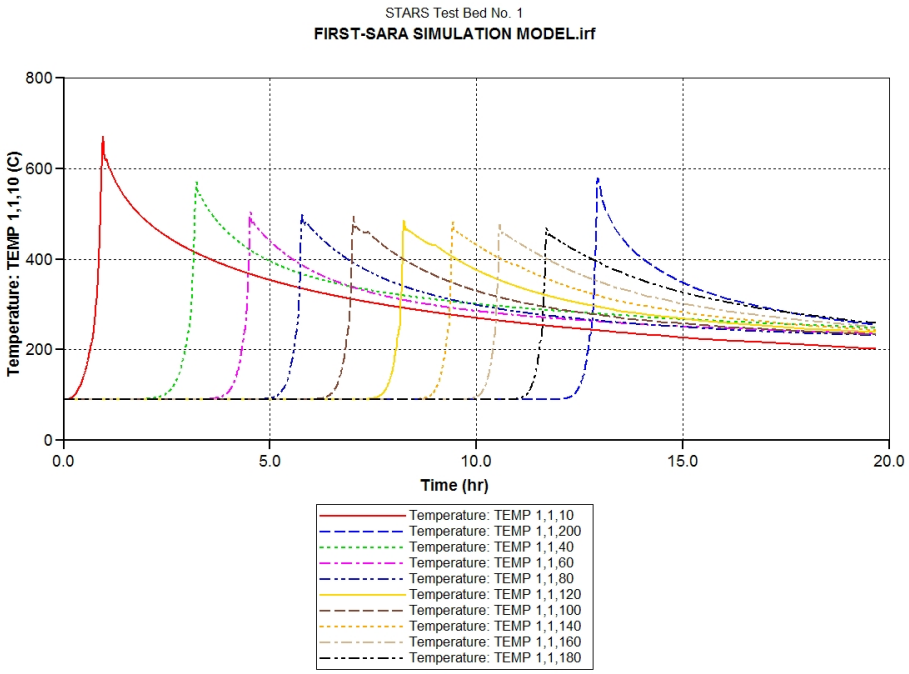

Figure 4-11: Temperature profile versus time of first SARA simulation model.

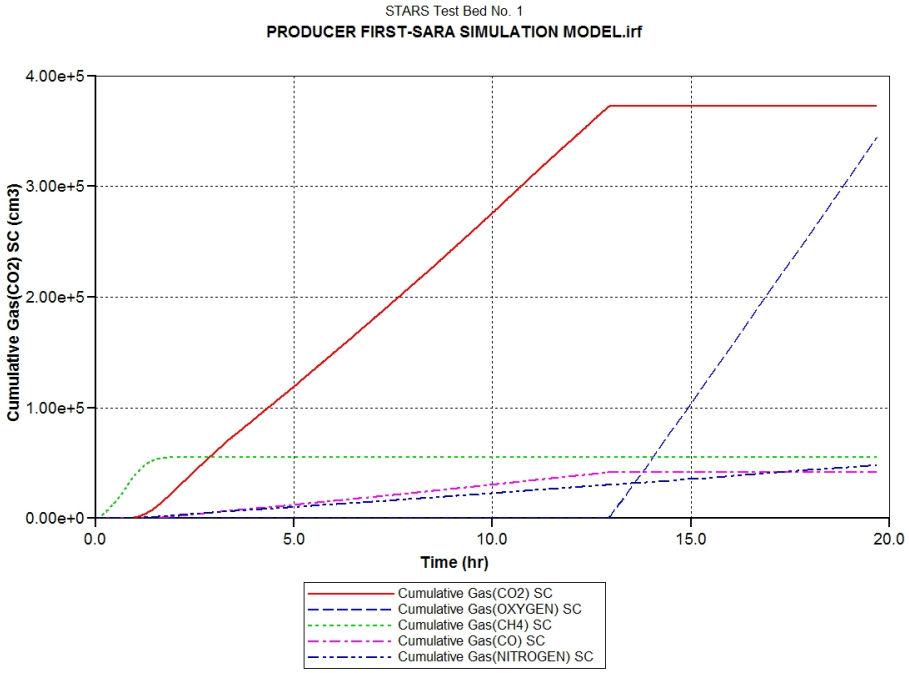

Figure 4-12: Cumulative gas component productions profile versus time for First SARA simulation model.

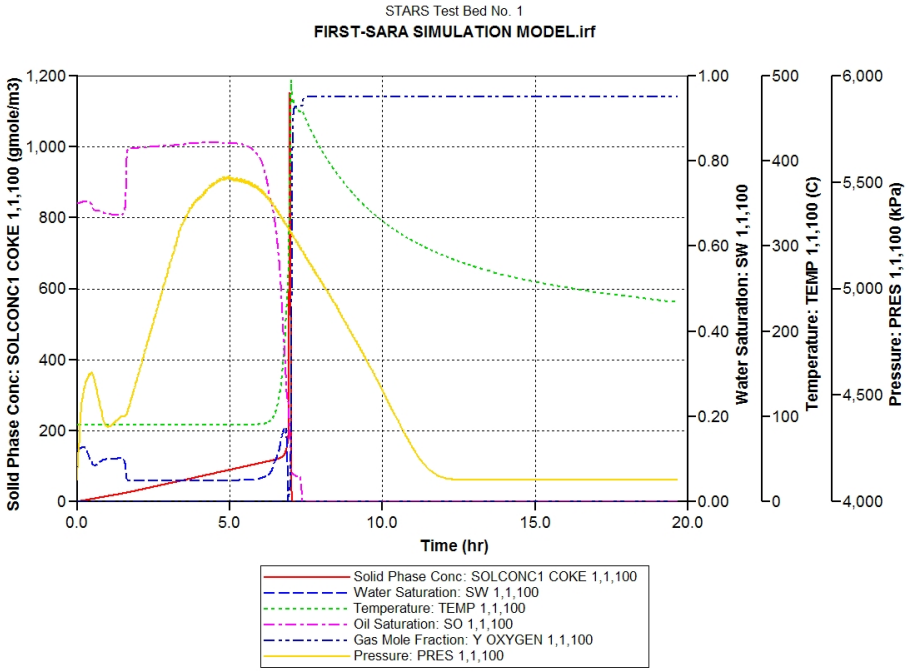

Figure 4-13: Coke concentration, water saturation, pressure, oil saturation, temperature, and oxygen mole fraction profile for First SARA simulation model.

4-1-4 SARA based simulation model

The 'First SARA simulations' showed that the chosen kinetic parameters give erroneous results, e.g., coke formation was already observed at low temperatures resulting in higher

temperatures in the combustion tube and early oxygen break-through. Consequently, the kinetic parameters were adjusted to match the simulation results of the main base case.

The combustion reaction rates can be increased either by increasing the frequency factor or decreasing the activation energy. The adjustment of the kinetic parameters of the SARA based simulations was based on the cumulative produced oil and gas of the minimal model (Main base case) as this was the only data available from experimental data. However, this was the first approach; therefore a more sophisticated method should be used for the adjustment of the kinetic parameters in a later work. The adjusted kinetic input parameters are given in Appendix A. Figure 4-14shows the cumulative oil and gas productions profiles obtained

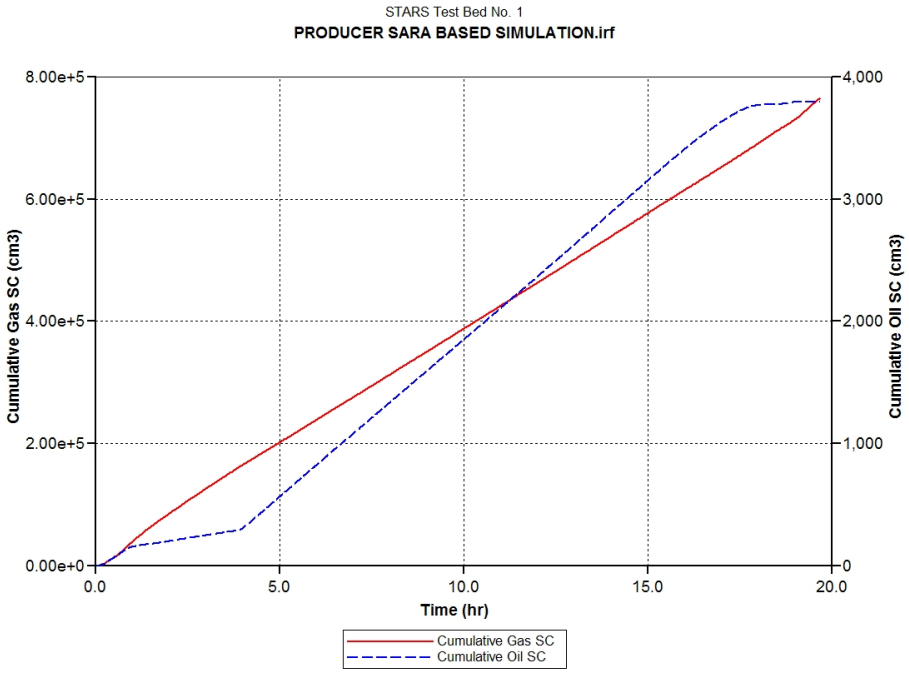

Figure 4-14: Cumulative oil and gas productions profile versus time for SARA based simulation.

from this simulation. The cumulative oil production could be matched nicely by adjusting the kinetic parameters. However, the gas production could not be described properly. A lower cumulative gas production at the same oil production was observed (see for comparison Figure 4-14 and Figure 4-1 of main base case). Figure 4-15 shows the temperature profiles versus time for the simulation describing the oil in terms of SARA fractions with adjusted kinetic parameters. Qualitatively, the temperature profiles show the same trend as for the base case simulations. However, the maximum temperatures reached in combustion tube are slightly higher, e.g., blocks (1 1 10) 727°C compared to block (1 1 10) 670°C for the main base case.

The slightly higher temperature is caused by a slightly higher coke production (see Figure 4-18). As it can be seen from the increasing methane concentration simultaneous with the increase of coke concentration (see Figure 4-17) coke was generated during cracking of the asphaltenes (see also chapter 2,equation (2-16)). Differently than for the first SARA simulations the coke production started now at realistic temperatures. As a consequence oxygen break-through occurs at later time, namely after 19.01 hours. Additionally, the higher tem-

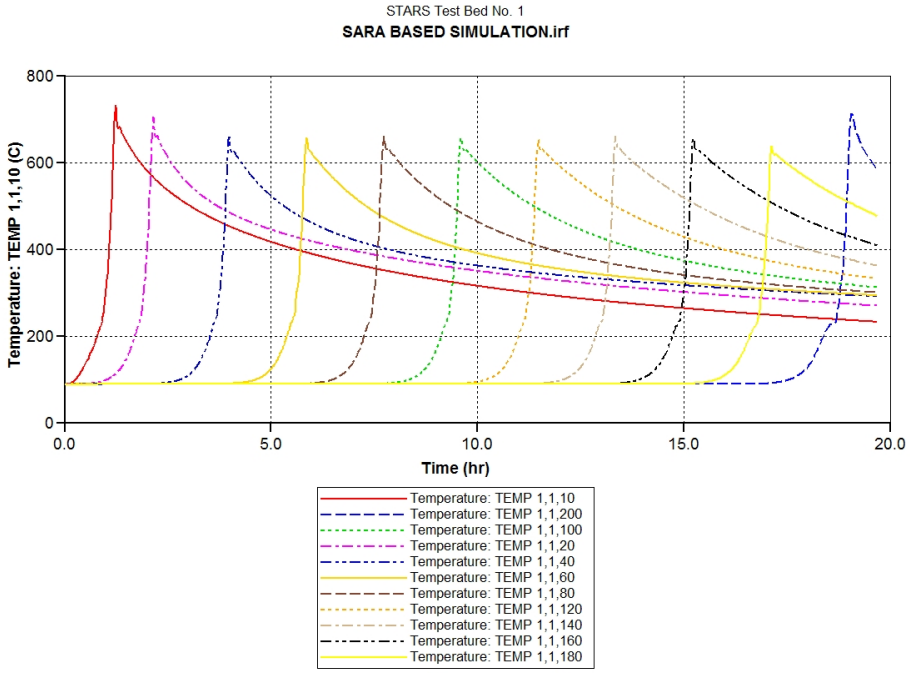

Figure 4-15: Temperature profile versus time of SARA based simulation model

peratures are caused by the combustion of hydrocarbon gases. This can be deduced from the fact that the carbon dioxide concentration still increases after constant cumulative oil production (See Figure 4-16 and Figure 4-14)

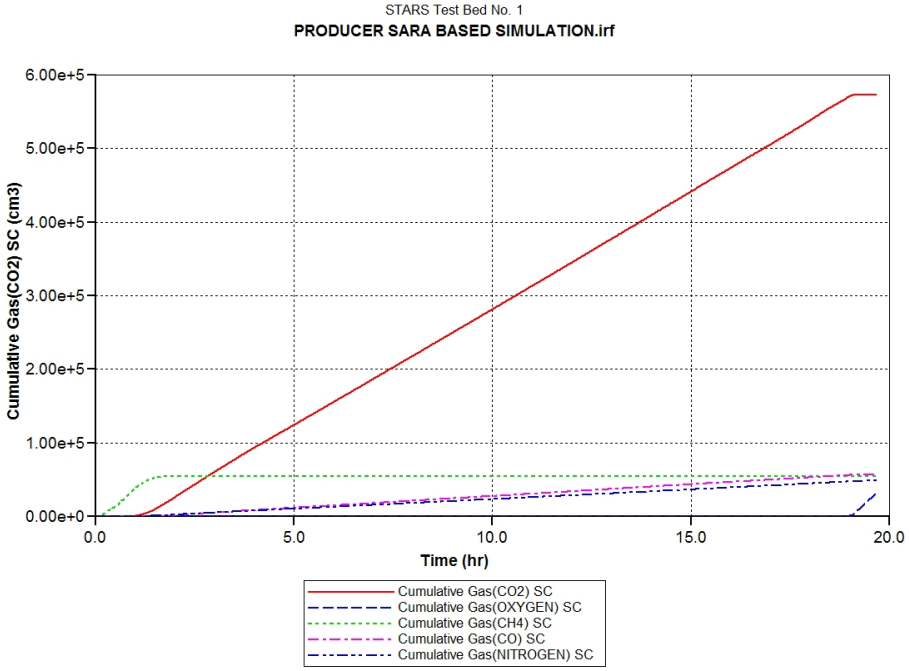

Figure 4-16: Cumulative gas component productions profile versus time for SARA based simulation model.

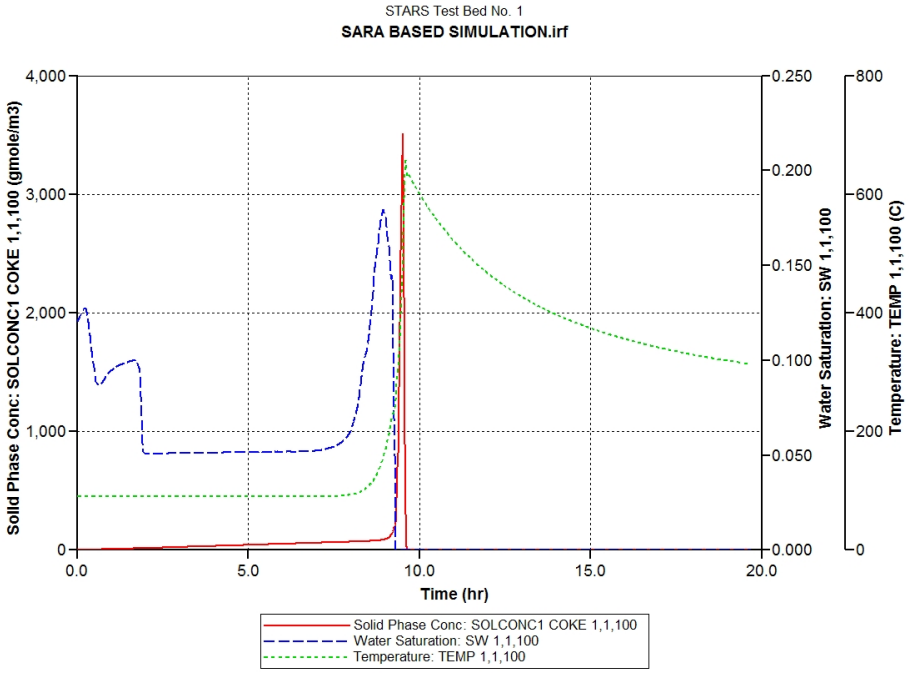

Figure 4-17: Coke concentration and water saturation profile of SARA based model

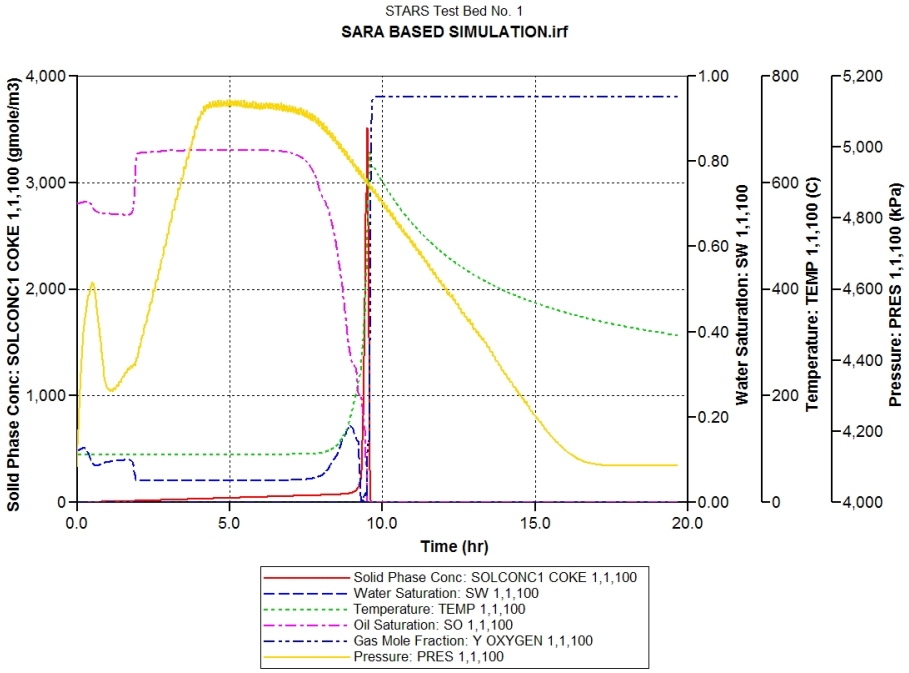

Figure 4-18: Coke concentration, water saturation, pressure, oil saturation, temperature, and oxygen mole fraction profile for SARA based model

Simulations	Activation energy	Liquid heat capacity	Gas heat capacity	Percentage of oxygen injection	Injection temperature
Main base case	Activation energy was adjusted to 5.31×10^4 for asphaltene LTO reaction			95% Enriched oxygen injected	400 °C was used to initiate ignition
Base case-1	Activation energy was adjusted to 4.3×10^4 for asphaltene cracking reaction and 3.95×10^4 for asphaltene LTO reaction			Linear increase of oxygen from 0 to 95% was injected	Temperature was varied from 400°C to 180 °C for 0.7 hrs
First SARA model	Initia kinetic data of the main base case was used.This was done by assigning the kinetic data of maltenes to aromatic and resins,while that of methane was used for saturates				
SARA based model	The first SARA based kinetic data was adjusted	A constant value of 2.10 was used	A zero(0) value was assigned		

Table 4-1: Adjusted simulations parameters

Chapter 5

Conclusion and Recommendations

5-1 Conclusion

A kinetic model based on a minimal (main base case) description of the oil and the chemical reaction scheme representing an in-situ combustion tube experiments with an Athabasca bitumen was successfully used to simulate the experimental data.The input parameters are taken from Yang and Gates and Belgrave et al, 1990. It was observed in the minimal model that coke production commences at too low temperatures.Analysis of the simulation results showed that this is as a result of too low activation energy of the asphaltene LTO reaction; consequently, the value of the activation energy was adjusted such that coke generation started at a temperature of 150 °C which is the typical temperature for minimal model when compared with the results from a simulation for which the oil was described more sophisticated.The description of the oil in this more sophisticated approach is based on the SARA pseudo-component fraction, and the reaction scheme was adjusted accordingly in-order to obtain a realistic model that closely resembles the behaviour as seen in combustion tube experiments.Analysis of the results reveals that the kinetic parameters are crucial for a good description; otherwise an early oxygen breakthrough and or too low temperatures are encountered as seen in the'First SARA simulation' results.

The model results based on the SARA description of the oil of the Athabasca bitumen was more realistic,and the reaction scheme used describes the behaviour of combustion tube experiments better than the minimal model.

5-2 Recommendations

A field scale simulation should be done; however,the up-scaling of various input parameters such as the kinetic parameters is difficult and needs to be studied separately. It is also recommended to use a more complicated ISC model to account for the physical and chemical

changes of the oil. Some of the required kinetic data can be obtained from RTO experiments [13]. It is also recommended that a more sophisticated approach should be used for the tuning of the kinetic data in a future work.

It is important to state here that ISC mechanisms are largely a function of oil composition and rock mineralogy. Thus, the extent of the chemical reactions between crude oil and injected air, as well as the heat generated depends on the rock oil-matrix system. Therefore, this should be taken into account for future work.

In this work, a zero value gas heat capacity and a constant liquid heat capacity value were used for saturates, aromatics and resins due to lack of literature data. In future work,it should be studied how to determine these parameters reliably.

Bibliography

[1] Political clashes shake venezuela's strained oil industry. *New York Times*. (Cited on page 1).

[2] P.Bakker A.H.de Zwart and C.A.Glandt. A thermal recovery for medium-heavy oil reservoirs. *SPE North Africa Technical conference and Exhibition held in Marrakech, Morocco*. (Cited on pages 2, 6, and 7).

[3] Nofal W.A. Ali, M.A. *Fuel Sci. Technol. Intl.*, 12:21, 1994. (Cited on page 12).

[4] N. Aske. Characterisation of crude oil components,asphaltene aggregation and emulsion stability by means of near infrared spectroscopy and multivariate analysis.ph.d. thesis, department of chemical engineering, norwegian university of science and technology,. (Cited on pages 12 and 13).

[5] Escalier J.-C Souteyrand C. Caude M. Rosset R. Bollet, C. *Journal of Chromatography.*, 206:289., 1981. (Cited on pages 12 and 18).

[6] S.A.Metha M.G.Ursenbach B.Sequera, R.G.Moore. Numerical simulation of in situ combustion experiments operated under low temperature conditions. *Journal of Canadian petroleum Technology*, 49. (Cited on pages 9, 17, and 19).

[7] W.E. Castanier, L.M.and Brigham. In situ combustion. society of petroleum engineers handbook, 2004. (Cited on page 7).

[8] W.A. Dark. *Journal of Liquid Chromatography*, 5:1645., 1982. (Cited on page 12).

[9] Hughes R. Dubdub, I. and D. Price. Kinetics of in situ combustion of athabasca tar sands studied in a differential flow reactor. *Chem. Eng. Res. Des.*, 68. (Cited on page 19).

[10] W.E. Brigham Fassihi, M.R. and H.J. Ramsey Jr. Reaction kinetics of in-situ combustion:part 1 observation, part 2 modeling. *Soc. of Pet. Eng. J.*, 24. (Cited on pages 14 and 19).

[11] Michael Fox. Venezuela increases taxes on oil companies in orinoco oil belt. (Cited on page 2).

[12] Sablotny D.M. Grizzle, P.L. *Analytical Chemistry*, 58:2389., 1986. (Cited on pages 12 and 18).

[13] M.G.Ursenbach D.W.Bennion. J.D.M.Belgrave, R.G.Moore. A comprehensive approach to in-situ combustion modelling. *SPE Advanced Technology Series*, 1, 1995. (Cited on pages 14, 19, and 44).

[14] C. Joseph and W.H. Pusch. A field comparison of wet and dry combustion. *Journal of Petroleum Technology,*. (Cited on page 9).

[15] F.David Martin Joseph J.Taber and R.S. Seright. Eor screening criteria revisited. a paper presented at the spe/doe tenth symposium on improved oil recovery held in tulsa, ok. *New Mexico Petroleum Recovery Research Center*. (Cited on pages 2 and 6).

[16] W.E. Brigham L.M. Castanier. Upgrading of crude oil via in situ combustion. *Journal of Petroleum Science and Engineering*, 39:125–136, 2003. (Cited on page 15).

[17] Greibrokk T. Lundanes, E. *Journal of High Resolution Chromatography.*, 17:197, 1994. (Cited on page 12).

[18] B.M.Sequera Marin. simulation of low temperature oxidation reactions of athabasca bitumen using sara fractions. *An MSc thesis Dept. of Chemical and Petroleum Engineering University of Calgary*. (Cited on page 19).

[19] Bennion-D. W. Belgrave J. D. M. Gie D. N. Moore, R. G. and M. G. Ursenbach. New insights into enriched-air in situ combustion. *J. Petrol. Technol.*, 42. (Cited on page 19).

[20] Per G.Thomsen. Michael.l. Michelsen. Erling H.Stenby Morten R.Kristensen., Margot.Gerristen. Efficient reaction integration for in-situ combustion simulation. *Transport in Porous Media*. (Cited on pages 1, 2, and 5).

[21] White P.D. Moss, J.T. and Jr. McNeil, J.S. In situ combustion process-results of a five well field experiment in southern oklahoma. *J.Pet.Technol.,*, 11. (Cited on page 19).

[22] National Energy of Canada. Candian energy overview. (Cited on page 1).

[23] Department of Energy USA. Country energy data. (Cited on page 2).

[24] Subodhsen Peramanu and Barry B. Pruden. Molecular weight and specific gravity distributions for athabasca and cold lake bitumens and their saturate, aromatic, resin, and asphaltene fractions. *Natural Resources Canada, Devon, Alberta, Canada T0C 1E0. Ind. Eng. Chem. Res.*, 38. (Cited on page 51).

[25] M. Prats. Thermal recovery, of spe monograph series,. *Society of Petroleum Engineers.*, 1986. (Cited on page 7).

[26] C.J. Laureshen SPE M.G.Ursenbach SPE S.A.Mehta and J.D.M.Belgrave R.G.Moore, SPE. Combustion/oxidation behaviour of athabasca oil sands bitumen. *SPE Reservoir Eva. and Eng.*, 2. (Cited on page 15).

[27] J.D.M.Belgrave M.G.Ursenbach R.G.Moore, C.J.Laureshen and S.A.R.Mehta. In situ combustion in canadian heavy oil reservoirs. (Cited on page 15).

[28] O.Kelvin meyers P.F. Baslle R.Mohammed Fassihi, SPE. Low temperature oxidation of viscous crude oils. (Cited on page 15).

[29] P.S. Sarathi. *In-situ combustion handbook–principles and practices.* United States Department of Energy, National Petroleum Technology Office. (Cited on pages 7, 8, 9, 10, 11, 12, 14, 16, 18, and 19).

[30] Aske N. Auflem I.H. Brandal O. Havre T.E. Saether O. Westvik A. Johnsen E.E. Sjoblom, J. and H Kallevik. Our current understanding of water in crude emulsions. recent characterization techniques and high pressure performance. *Norwegian University of Science and Technology (NTNU).* (Cited on page 13).

[31] O.P.and lown E.M. Strausz. The chemistry of alberta oil sands,bitumens and heavy oils. *Alberta:Alberta Energy Research Institute(AERI),Calgary,.* (Cited on pages 13 and 18).

[32] J.C. Trantham and J.W. Marx. Bellamy field tests: Oil from tar by counterflow underground burning. *Journal of Petroleum Technology.* (Cited on page 12).

[33] Y.Xiaomeng and .I.Gates. Combustion kinetics of athabasca bitumen from 1d combustion tube experiments. *Natural Resources Research*, 18. (Cited on pages 16, 19, and 20).

Appendix A

Appendix

The following parameters;viscosity,equlibrium k-value,components distribution phases,gas and liquid heat capacities,molecular weight and kinetic data given in tables A-1 to table A-8 were used for the 'First SARA simulation' and for the 'SARA based simulation'.

Component	$Avisc$	$Bvisc$	Avg	Bvg
Saturates[1]	1.227×10^{-4}	4309.413	1.057×10^{-4}	0.82
Aromatics[1]	1.3031×10^{-3}	4148.488	2.46×10^{-4}	0.466
Resins[1]	12.0554	3353.48	2.46×10^{-4}	0.466
Asphaltenes[2]	4.892×10^{-25}	33147	1.0573×10^{-4}	0.82
H_2O_2[2]	4.7352×10^{-3}	1515.7	2.16×10^{-5}	1.076
O_2[2]			-3.355×10^{-1}	0.720
HydrocarbonGas[2]	1.32383×10^{-2}	1005.5	-1.07×10^{-4}	0.8655
CH_4[2]	1.04328×10^{-2}	262.82	1.0573×10^{-4}	0.80
CO_2[2]	1.40×10^{-3}	2544	1.07×10^{-4}	0.823
CO[3]	1.19257×10^{-2}	216.58	3.0×10^{-4}	0.796
N_2[3]			3.0×10^{-4}	0.347

Table A-1: SARA base liquid viscosity
[1](Morten), [2](Yang and Gates, 2009)

Component	K_{v1}	K_{v4}	K_{v5}
Saturates	8.365×10^7	-9874.8	-273
Aromatics	9.91×10^7	-10968.6	-273
Resins	6.39×10^8	-15860	-273
Asphaltenes	0	0	0
Water	1.18×10^7	-3820	-227
Hydrocarbon Gas	8.62×10^8	-3100	-273
CH4	5.45×10^5	-879	-266
CO2	8.62×10^8	-3100	-273
CO	2.32×10^5	-530	-260

Table A-2: SARA base gas liquid K-value
[1]CMG STARS(Winprop) [2]Yang and Gates,2009

Components	Oil	Gaseous	Aqueous	Solid
Water		X	X	
Saturates	X	X		
Aromatics	X	X		
Resins	X	X		
Asphaltenes	X			
Oxygen		X		
Nitrogen		X		
Hydrocarbon gas	X			
Carbon II Oxide	X			
Carbon iv Oxide	X			
Methane	X	X		
Coke				X

Table A-3: SARA based phase distribution of components

Gas heat capacity Correlations:$C_{pg}(J/gmol°C) = C_{pg1} + C_{pg2}T^2 + C_{pg3}T^3$

Component	C_{pg1}	C_{pg2}	C_{pg3}	C_{pg4}
Saturates[1]	0	0	0	0
Aromatics[1]	0	0	0	0
Resins[1]	0	0	0	0
Asphaltenes[2]	0	0	0	0
O_2[2]	28.1	-3.68×10^{-6}	1.75×10^{-5}	-1.06×10^{-8}
HydrocarbonGas[2]	19.8	7.34×10^{-2}	-5.60×10^{-5}	1.71×10^{-8}
CH_4[2]	19.3	5.21×10^{-2}	1.20×10^{-5}	-1.13×10^{-8}
CO_2[2]	19.8	7.34×10^{-2}	5.60×10^{-5}	1.71×10^{-8}
CO[2]	30.9	-1.29×10^{-2}	2.79×10^{-5}	-1.27×10^{-8}
N_2[2]	31.2	-1.36×10^{-2}	2.68×10^{-5}	-1.17×10^{-8}

Table A-4: SARA base gas liquid heat capacity
[1](Morten), [2](Yang and Gates, 2009)

Liquid heat Capacity Correlations:$C_{pl}(J/gmol°C) = C_{pl1} + C_{pl1}T + C_{pl3}T^2 + C_{pl4}T^3$

Component	C_{pl1}	C_{pl3}	C_{pl3}	C_{pl4}
Saturates[1]	2.10	0	0	0
Aromatics[1]	2.10	0	0	0
Resins[1]	2.10	0	0	0
Asphaltenes[2]	2510	0	0	0
O_2[1]	46.4	-3.95×10^{-1}	-7.05×10^{-3}	3.99×10^{-5}
HydrocarbonGas[1]	-3980	5.25×10^{-1}	-2.27×10^{-1}	3.29×10^{-4}
CH_4[2]	-0.02	1.20	-9.87×10^{-3}	3.17×10^{-5}
CO_2[2]	-3890	5.25×10^{1}	-2.27×10^{-1}	3.29×10^{-4}
CO[2]	126	-1.70	1.70×10^{-2}	4.19×10^{-6}
N_2[2]	76.5	-3.52×10^{-1}	2.67×10^{-3}	5.01×10^{-5}

Table A-5: SARA based Liquid heat capacity
[1] Morten et al. [2]Yang and Gates, 2009,

Component	Molecular Weight	Critical Temperature Tc	Critical Pressure Pc
	[g/mol]	°C	[KPa]
Saturates[1]	381	593	933
Aromatics[1]	408	686	1071
Resins[1]	947	850	1480
Asphaltenes[1]	2005	1126	253
Coke[2]	13.1	-	-
Water[2]	18.0	374	22,100
O_2[2]	32.0	-119	5050
Gas[2]	100	267.05	2736
CH_4[2]	16.0	-82.6	4600
CO_2[2]	44.0	31.1	7380
CO[2]	28	-140	3490

Table A-6: Molecular weight and critical properties of SARA based
[1]Peramau et al [24]. [2]Yang and Gates,2009 [3]CMG STARS(Winprop) [2]Yang and Gates,2009

Parameter	Value
Initial water saturation	0.12
Initial oil saturation	0.70
Initial gas saturation	0.18
Initial bitumen mole fraction-Saturates	0.254
Initial bitumen mole fraction-Aromatics	0.545
Initial bitumen mole fraction-Resins	0.152
Initial bitumen mole fraction-Asphaltenes	0.049

Table A-7: First SARA and SARA based simulations initial conditions(Peramau *et al.* (1999))

Reaction	A	Ea	Hr
	Frequency factor	Activation Energy	Heat of reaction
		[J/mol]	[J/mol]
10	$1.12 \times 10^{13} day^{-1}$	1.16×10^{6}	0
11	$6.20 \times 10^{13} day^{-1}$	4.02×10^{4}	0
12	$1.82 \times 10^{4} day^{-1}$	1.76×10^{5}	0
13	$2.01 \times 10^{14} day^{-1}$	1.76×10^{5}	0
14	$1.05 \times 10^{8} day^{-1}$	1.70×10^{5}	1.81×10^{6}
15	62393	4.05×10^{4}	2.26×10^{6}
16	$62969.9 day^{-1} KPa^{-0.4246}$	3.45×10^{4}	2.77×10^{6}
17	$6.02 \times 10^{7} day^{-1} KPa^{-1}$	1.05×10^{5}	1.68×10^{6}
18	$9296 day^{-1} KPa^{-1}$	6.84×10^{4}	4.78×10^{5}
19	$1.31 \times 10^{8} day^{-1}$	2.66×10^{5}	4.44×10^{5}
20	$3.02 \times 10^{10} day^{-1} KPa^{-1}$	5.95×10^{4}	8.91×10^{5}

Table A-8: SARA based kinetic data

Appendix B

Nomenclature

A:	frequency factor	[ ]
E_a:	activation	[J/mole]
T:	temperature	[K]
T_c:	critical temperature	[K]
P_c:	critical pressure	[Pa]
P:	pressure	[Pa]
R:	universal gas constant	[J/mole K]
k:	reaction rate constant	[ ]
$Visg$:	combined gas viscosity of all component i	[Pa.s]
$Visg\{\text{i}\}$:	gas viscosity of component i	[Pa.s]
$Avg\{\text{i}\}$:	first coefficient in correlation for tempearture dependence of viscosity of component i in the gas phase	[Pa.s]
$Bvg\{\text{i}\}$:	second coefficient in correlation for tempearture dependence of viscosity of component i in the gas phase	[Pa.s]
$Avisc$ and $Bvisc$:	coefficients of the correlation for temperature dependence of component viscosity in the liquid phases	[Pa.s]
COFCAW:	Combination of forward combustion and water flooding	[ ]
SARA:	saturates,aromatics,resins,asphaltenes	[ ]
$y\{i\}$:	mole fraction of gas component i	[ ]
HTO:	high temperature oxidation	[ ]
LTO:	low temperature oxidation	[ ]
μ_{malt}:	viscosity of maltene	[Pa.s]
μ_{asp}:	viscosity of asphalatene	[Pa.s]